The effects of μ-opioid receptor agonists on respiratory neurons in the preBötzinger complex in decerebrate dogs

Mustapić, Sanda

UNIVERSITY OF SPLIT
SCHOOL OF MEDICINE

Sanda Mustapić, M.D.

THE EFFECTS OF μ-OPIOID RECEPTOR AGONISTS ON RESPIRATORY NEURONS IN THE PREBÖTZINGER COMPLEX IN DECEREBRATE DOGS

DOCTORAL THESIS

Split, 2013.

UNIVERSITY OF SPLIT
SCHOOL OF MEDICINE

Sanda Mustapić, M.D.

THE EFFECTS OF μ-OPIOID RECEPTOR AGONISTS ON RESPIRATORY NEURONS IN THE PREBÖTZINGER COMPLEX IN DECEREBRATE DOGS

DOCTORAL THESIS

Mentor: Professor Edward J. Zuperku, Ph.D.

ABBREVIATIONS

5-HT – serotonin

aCSF – artificial cerebrospinal fluid

BötC – Bötzinger complex

BPM – breaths per minute

cAMP – cyclic adenosine monophosphate

CNS – central nervous system

cVRG – caudal part of the ventral respiratory column

DAMGO – [D-Ala2, N-Me-Phe4, gly-ol5]-enkephalin

DLH – D-homocysteic acid

E – Aug – expiratory augmenting

E –Con – expiratory constant

E – Dec – expiratory decrementing

E – expiratory

EM 1 and EM 2 – endomorphin types 1 and 2

f_B – frequency breathing

GPCR – G protein coupled receptors

I – Aug – inspiratory augmenting

I_{CAN} – calcium-activated non-selective cationic current

I – Con – inspiratory constant

I – Dec – inspiratory decrementing

I – inspiratory

KF – Kolliker Fuse nucleus

kPa – kilo Pascal

MOR – μ-opioid receptors

NAL – naloxone

NTS – nucleus of the solitary tract

PBN – parabrachial nuclei

PKA – protein kinase A

PNG – phrenic neurogram

PPA – peak phrenic activity

preBötC – preBötzinger complex

remi – remifentanil

RTN – retrotrapezoid nucleus

rVRG – rostral part of the ventral respiratory column

T_E – expiratory time

T_I – inspiratory time

TRH – thyrotropin releasing hormone

VRC – ventral respiratory column

Contents

1. INTRODUCTION

Breathing is a primal homeostatic neural process, regulating levels of oxygen and carbon dioxide in blood and tissues, which are crucial for life. Rhythmic respiratory movements must occur continuously throughout life and originate from neural activity generated by specially organized circuits in the brainstem. Aggregates of respiratory neurons that discharge periodically during breathing are distributed bilaterally in the bulbar brainstem, from the rostral pons to the caudal border of the medulla. Synaptic interactions among respiratory neurons establish the network respiratory rhythm, and their connections with cranial and spinal motoneurons and interneurons set up the timing and pattern of contraction in the muscles of respiration (1).

1.1. Respiratory neurons

Respiratory inspiratory (I) and expiratory (E) neurons are usually categorized by their characteristic augmenting (I-Aug, E-Aug), decrementing (E-Dec, I-Dec) or relatively constant (E-con, I-Con) firing patterns, and by firing patterns that either span the boundaries between inspiratory and expiratory phases (E-I, I-E) or which fire only during subportions of the respiratory phases. It should be appreciated that within the ventral respiratory column (VRC) a given phasic firing pattern may not be uniquely associated with a given excitatory or inhibitory transmitter (2).

Respiratory neurons of the brainstem receive modulatory synaptic input from non-respiratory regions such as the motor cortex, pontine and medullary reticular formations, cerebellum, hypothalamus, other limbic and cardiovascular regions of the brainstem as well as from extrapyramidal motor areas. These non-respiratory modulatory inputs adapt breathing rhythm and pattern for effective cardio-respiratory interactions and activities such as phonation, swallowing, coughing, physical exertion, defecation and postural change (1).

Respiratory neurons are concentrated in three main brainstem areas: the dorsal respiratory group within the nucleus of the solitary tract, the ventrolateral medulla from the level of the spinal-medullary junction through the level of the facial nucleus (i.e. VRC) and in the pontine parabrachial-Kölliker-Fuse complex within the dorsolateral pons. The latter neurons are

referred to as the pontine respiratory group (PRG). These aggregates of brainstem respiratory neurons are interconnected, and together with respiratory-related sensory afferents, are collectively responsible for the automatic control of breathing as well as adaptive changes in breathing to homeostatic and environmental challenges.

1.1.1. The dorsal respiratory group

The dorsal respiratory group is identified with respiratory neurons (mainly inspiratory) concentrated in the ventrolateral subnucleus of the nucleus of the solitary tract (NTS). The caudal third of the nucleus of the solitary tract (cNTS) is also the site of one of three principal concentrations of brainstem respiratory neurons, the "dorsal respiratory group". As the main focus for the mainly topographic sensory terminations of pulmonary and airway afferents traveling in the vagus and glossopharyngeal nerves, it provides the first step in the brain's processing of critical information about the status of lungs and airways, as well as sensory input from peripheral chemoreceptors detecting arterial O_2 and CO_2. NTS appears to include glutamate as a transmitter, often together with a monoamine, purine, peptide or volatile cotransmitter.

1.1.2. The ventral respiratory column

The respiratory network in the ventrolateral medulla is referred to as the ventral respiratory column (VRC) in groups designated from caudal to rostral as the caudal ventral respiratory group (cVRG), the rostral ventral respiratory group (rVRG), the preBötzinger complex (preBötC), the Bötzinger complex (BötC), the parafacial respiratory group (pFRG) and the retrotrapezoid nucleus (RTN) (3).

The VRC occupies the ventrolateral medulla along its entire length and is populated by various types of respiratory neurons identified by their activation during the inspiratory or expiratory phase of the respiratory cycle. Respiratory rhythm generation occurs mainly as a result of circuit interactions in the rostral half of the VRC. Bulbospinal neurons in the caudal half of the VRC transmit this rhythm unchanged but their activity modulates the amplitude of respiratory motor output on spinal respiratory nerves. Within the VRC respiratory neurons form a sequential series of compartments (2).

1.1.2.1. Rostral and caudal divisions of the ventral respiratory group

In the caudal half of the medulla a "ventral respiratory group" (VRG) was initially identified and subdivided into rostral (rVRG) and caudal (cVRG) portions based on the prominence of inspiratory (I) neurons in rVRG, and expiratory (E) neurons in cVRG (2). cVRG beginning at the level of the obex just to the nucleus ambiguous and extending to the spinal medullary border, contains several different types of neurons with respiratory related activity. Most of the neurons found in the cVRG with a firing pattern that increases during expiration are excitatory premotor neurons projecting to the ventral horn neurons controlling abdominal and other expiratory muscles (3).

The rVRG contains the main aggregate of excitatory (glutamatergic) bulbospinal inspiratory neurons (I-Aug). These neurons project monosynaptically to inspiratory motoneurons in the phrenic nucleus in the cervical spinal cord that innervate the diaphragm, and to external intercostal motoneurons in the thoracic spinal cord (4,5). rVRG and cVRG neurons are responsible for activation of inspiratory and expiratory pump muscles, and at least for bulbospinal I-Aug neurons, glutamate and enkephalin are likely co-transmitters (6).

The anterior portion of the rVRG also harbors a unique population of NK1 receptor positive I-Aug glutamatergic bulbospinal neurons. These neurons are distinguished from other I-Aug rVRG neurons by their expression of NK1 receptors and by modest differences in their firing pattern (5). Bulbospinal NK1 receptor positive propriobulbar neurons in the preBötC by their spinal projections and larger size (5,7), as well as by their I-Aug firing pattern as compared to the E-I pattern common in preBötC neurons (2).

1.1.2.2. Rostral VRC: Bötzinger, preBötzinger, retrotrapezoid nucleus, and the parafacial respiratory group

The rostral half of the VRC, while participating in determining the pattern or envelope of activity on respiratory nerves, additionally encompasses neuronal populations that are the main source of respiratory rhythm generation (8,9). rVRG neurons related to respiratory rhythm formation are located in several adjacent compartments, including the most anterior portions of the rVRG, the preBötC, and possibly elements of the RTN. The rVRG includes substantial

populations of respiratory neurons that project locally within the brainstem and particularly within the medulla (2).

1.1.2.2.1. The Bötzinger complex

The BötC was initially discriminated by the presence of a prominent population of expiratory neurons in the region immediately caudal to the facial nucleus providing afferents to the NTS of the cat. BötC expiratory neurons have subsequently been intensively examined and shown to provide widespread inhibitory projections within the VRC with E-Aug neurons targeting both inspiratory and expiratory bulbospinal neurons as well as substantial numbers of respiratory-related cranial motoneurons (2). Some of the E-Aug BötC neurons also project via axon collaterals to the spinal cord, reaching at least as far as the phrenic nucleus (10). A subset of BötC neurons send axons rostrally, targeting the facial nucleus and RTN, and appear to target further respiratory-related areas of the pons. In the rat, both E-Aug and E-Dec BötC neurons have been shown to use glycine as a transmitter (11). In the dog, GABAergic inputs to inspiratory bulbospinal neurons appear to predominate over glycinergic afferents during the expiratory phase of breathing (12); the BötC is one of the most likely sources of such expiratory inhibitory afferents (2). The BötC neurons are critically involved in the control of the transition between inspiratory and expiratory activities in the network, which is fundamental for the rhythmic inspiratory-expiratory alternation essential for normal breathing (13).

1.1.2.2.2. The preBötzinger complex

The preBötC was identified in vitro as a medullary region essential for respiratory rhythm generation (14). Situated between the BötC and rVRG, the preBötC demonstrates peak populations for neurons whose in vivo firing patterns span the temporal boundaries between the expiratory and inspiratory phases of the respiratory cycle (15).

PreBötC circuits can express autorhytmic or pacemaker-like activity that generates a rudimentary pattern of inspiratory activity when the structure is experimentally isolated *in vitro* (16,17). Isolated in medullary slices, the preBötC continues to generate three distinct types of

activity patterns that appear to provides the basic rhythmic drive for the generation of three distinct forms of respiratory activity patterns: normal respiratory activity, sighs and gasps (18).

Autorhytmic or pacemaker-like activity is proposed to be based on excitatory synaptic interactions within the preBötC and intrinsic cellular mechanisms involving persistent sodium current (13). The intrinsic rhythm activity of the network may also involve calcium-activated non-selective cationic current (I_{CAN}), which in combination with excitatory synaptic interactions can also provide cellular and network level rhythmic bursting (19,20). These and other neuronal currents and excitatory synaptic interactions provide mechanisms for regenerative initiation, maintenance and termination of inspiratory network activity in the isolated preBötC *in vitro.* PreBötC circuits serve two basic functions: a) generation of rhythmic excitatory inspiratory drive, including the pre-I component of this drive that is important for initiation of the inspiratory phase and b) coordination of inspiratory-expiratory pattern formation via inspiratory inhibition provided by the preBötC inhibitory neurons (13).

The preBötC is connected with many other neuronal networks that are themselves under continuous modulatory control. Respiratory rhythm generating areas, such as the preBötC receive multiple modulatory inputs from many areas outside and within the vicinity of the preBötC. The preBötC projects to various respiratory-related areas that contain neuromodulators and are in turn modulated by multiple other areas. Regions that are well known for their important modulatory roles are raphe magnus and obscures. These regions contain a variety of neurotransmitters and neuromodulators including GABA, serotonin (5-HT), substance P and thyrotropin releasing hormone (TRH) (21).

All these areas either receive input from or project to the preBötC (22). Within the preBötC, substance P is primarily co-localized with glutamate, but to lesser degree also with GABA (23). By acting on different receptors and neurons opioids exert differential inhibitory effects on the frequency of respiratory activity. The frequency effects seem to be mediated in part by neurons within the preBötC since μ-opioid receptor agonists inhibit respiratory activity when injected directly into the preBötC (24). Inspiratory neurons located within the preBötC exhibit two types of pacemaker properties. Pacemaker bursting in one population of inspiratory neurons seems to depend on the I_{CAN}. These neurons are referred to as “cadmium-sensitive” pacemaker neurons, because bursting in these neurons is abolished following blockade of calcium influx with

extracellularly applied cadmium. Pacemaker bursting in the other population of inspiratory neurons seems to depend on the persistent sodium current. These neurons are referred to as "cadmium-insensitive" pacemaker neurons, because bursting in these neurons continues even following blockade of calcium currents with extracellularly applied cadmium. Neuromodulators that cause a frequency and regularity increase in respiratory network activity evoke a frequency increase specifically in the endogenous bursting of isolated cadmium-insensitive pacemakers. Under normal conditions the two types of pacemaker neurons are active and excitatory and inhibitory synaptic mechanisms are critical for rhythm generation (21).

1.1.2.2.3. The retrotrapezoid nucleus/the parafacial respiratory group

Neuronal clusters that constitute the retrotrapezoid nucleus (RTN) and the parafacial respiratory group (pFRG) are located below and extend through the rostro-caudal levels of the facial motor nucleus. The pFRG/RTN contains neurons whose activity is sensitive to the brain carbon dioxide level and also receives input from peripheral, oxygen-sensitive chemoreceptors. The RTN provides chemosensitive excitatory drives to most of the respiratory network and adapts the activity to the metabolic state of system (13).

1.1.3. Pontine respiratory group

The VRC extends rostrally into the lateral pons as a nearly uninterrupted corridor of neurons interconnected with the VRC (2). The group of respiratory related neurons located in the pons around the parabrachial nucleus (PBN) and including the Kolliker Fuse (KF) nucleus is called the pontine respiratory group (PRG). Pontine conections to the caudal medullary circuits appear to be critical for coordinating the activity of expiratory muscles and upper airway musculature during expiration and for expression and regulation of post-inspiratory (post-I) activity. The major respiratory-related projections to this area are from NTS and from the VRC (25). The KF is the source of the most massive projections to the VRC, and additional projections to the respiratory-related areas of the NTS, as well as to the hypoglossal and facial nuclei (26).

1.2. The opioids

Morphine and synthetic μ-opioids are the most effective analgesics used for the control of acute and chronic pain. The analgesic properties of the opium poppy Papaverum somniferum were first mentioned by Hippocrates around 400 BC, and opioid analgesics remain the mainstay of pain management today. The most widely recognized and potentially fatal acute side-effect of opioid analgesics is respiratory depression, and this is of particular concern when opioid drugs are abused. Yet despite this serious problem, the key sites in the brain where opioid analgesics act to suppress breathing have not been identified (27,28).

The opioids are used in a wide variety of clinical situations, for example, after surgery and in cancer pain control. The incidence of postoperative opioid-induced respiratory depression in the UK has been estimated to be approximately 1% (29).

The opioid system regulates numerous physiological functions, including responses to stress, respiration, gastrointestinal transit, as well as endocrine and immune functions. It also plays a key role in modulating mood and well-being, as well as addictive behaviors (30). The effect of opioids ultimately depends on the expression of specific receptors.

1.2.1. The opioid receptors

Opioid receptors are broadly expressed throughout the brain, primarily in the cortex, limbic system and brain stem. Current consensus describes four classes of opioid receptors: the MOP (μ), KOP (κ), DOP (δ), and the nociceptin/orphanin FQ peptide receptor (NOP). The endogenous ligands for these receptors include the endorphins (MOP), enkephalins (DOP and MOP), the dynorphins (KOP), and nociceptin/orphanin FQ (NOP) (27).

Endogenous opioid peptides are small molecules that are naturally produced in the central nervous system (CNS) and in various glands throughout the body, such as the pituitary and adrenal glands. These peptides produce the same effects as the chemicals known as classic alkaloid opiates, which include morphine and heroine. Endogenous opioid peptides function both as hormones and as neuromodulators (31).

The endogenous opioid system mediates many physiological effects, including pain, respiratory control, stress responses, appetite, and thermoregulation. Opioid receptors are present in multiple non-respiratory sites around the body, and they are abundant in respiratory control centers that include the brainstem and higher centers such as the insula, thalamus and anterior cingulate cortex. Opioid recpetors are also located in the carotid bodies and in the vagi. Mechanosensory receptors located in the epithelial, submucosal, and muscular layers of the airways relay mechanical and sensory information from the lungs and express opioid receptors (27). Immunoreactivity for μ, δ and κ-receptors is found in respiratory-related regions of the brain stem and spinal cord (1). Binding sites for the three opioid receptors overlap in most structures, but some structures exhibit higher expression of one receptor over the others. MOR is the most expressed opioid receptor in the amygdale, thalamus, mesencephalon and some brainstem nuclei. μ and κ coexist in most structures, whereas the of δ is more restricted (low expression in the hypothalamus, thalamus, mesencephalon, and brainstem) (30).

1.2.2. G protein coupled opioid receptors

All four opioid receptors are seven transmembrane spanning proteins that couple to inhibitory G proteins. Stimulation by agonists activates the G-proteins tethered to the inner surface of the cell membrane and initiates an intracellular signaling cascade that mediates the actions of many hormones and neurotransmitters (27). When a G protein coupled receptor (GPCR) agonist binds to the extracellular domain, it induces a change in conformation of the receptor. This, in turn, leads to coupling to and activation of one or more G proteins inside the cell. The G proteins consist of three subunits: α, β and γ. Almost all GPCR agonists that have an analgesic action are coupled to $G_{i/o}$ proteins. GPCRs regulate the function of ion channels, which play an essential role in the function of neurons by mediating electrical currents and regulation of selective ion concentrations across the cell membrane (32).

After being activated by an agonist, such as the endogenous μ-opioid peptide endomorphin, or exogenous agonists, such as morphine and fentanyl, the G_{α} and $G_{\beta\gamma}$ subunits dissociate from one another and subsequently act on various intracellular effector pathways. GTPase activity is stimulated by opioid agonists and endogenous opioid peptides. Agonist stimulation of opioid receptors was also shown to inhibit cyclic adenosine monophosphate (cAMP) production in a

manner similar to that of other types of GPCR. When pertussis toxin was used to selectively adenosine diphosphate (ADP)-ribosylate the G protein, the inhibitory function of opioid receptors on cAMP signaling was found to be $G_{\alpha i}$ dependent.

The classic and perhaps most important aspect of opioid receptor signal transduction relates to opioids' ability to modulate calcium and potassium ion channels. After $G_{\alpha i}$ dissociation from $G_{\beta\gamma}$, the G_{α} protein subunit moves on to directly interact with the G-protein gating inwardly rectifying potassium channel, Kir3. Channel deactivation happens after GTP to guanosine diphosphate hydrolysis and $G_{\beta\gamma}$ removal from interaction with the channel. This process causes cellular hyperpolarization and inhibits tonic neural activity. In several reports, the inhibitory effects of opioids on neural excitability were shown to be mediated by interactions of opioid receptors with Kir3.

When activated, all four opioid receptors cause a reduction in Ca^{2+} currents that are sensitive to P/Q-type, and L-type channel blockers. Opioid receptor-induced inhibition of calcium conductance is mediated by binding of the dissociated $G_{\beta\gamma}$ subunit directly to the channel. This binding event is thought to reduce voltage activation of channel pore opening. Numerous studies have shown that opioid receptors interact with and modulate Ca^{+2} channels; this has led to the examination of specific Ca^{+2} channel subunits that may be involved in opioid receptor modulation. For instance, it was reported that MOR stimulation results in G protein-dependent inhibition of α_{1A} and α_{1B} subunits. Because the activation of μ, δ and κ opioid receptors inhibits adenyl cyclase activity, the cAMP-dependent Ca^{2+} influx is also reduced (33).

1.3. Possible sites for opioid-induced respiratory depression

As mentioned previously, systemic administration of μ-opioids at clinical doses for analgesia typically produces bradypnea during sedation and sleep (1). It has been proposed that μ-opioid receptors (MORs) on preBötC neurons, the putative kernel of respiratory rhythmogenesis, are responsible for the opioid-induced respiratory depression (24). Studies in brain slices that contain the preBötC show that μ-opioids markedly slow the burst rate of respiratory-related output (24,34) and produce slowing that has been characterized as quantal in neonatal rat brainstem-spinal cord preparations (35). Perturbations of neuronal function within the preBötC of adult animals severely disrupt breathing (36-38). In vivo studies using multibarrel

micropipettes and microiontophoresis have shown that localized application of μ-opioids on medullary respiratory neurons causes a decrease in neuronal discharge and membrane hyperpolarization, demonstrating the presence of functional MORs on these neurons (39,40).

Further evidence in support of the preBötC region as the site of the opioid induced depression of breathing rate is suggested by the co-expression of 5-HT_{4a} and MOR receptors in the preBötC and the ability of a 5-HT_{4a} agonist to reverse most of the opioid effect on breathing rate without reversing analgesia (41). The underlying mechanism for this functional antagonism was hypothesized to act by counterbalancing the opioid-induced decrease in intracellular cAMP via an increase in cAMP produced by activation of 5-HT_{4a} receptors. The functional antagonism did not affect the antinociceptive action of opioids, presumably because 5-HT_{4a} receptors are absent in the regions of the spinal cord involved in the processing of pain stimuli. Similarly, a study by Lalley (42) demonstrated that selective D1-dopamine receptor agonists, which are known to activate the cAMP-protein kinase A (PKA) signaling pathway in a variety of neurons, restored phrenic nerve activity after it had been abolished by the selective MOR agonist fentanyl in anesthetized and unanesthetized decerebrate cats. Again, it was suggested that the potential site of action could be on preBötC respiratory neurons.

In a recent study using the picoinjection technique combined with extracellular single-unit recording (27,43), we found that respiratory bulbospinal premotor neurons in decerebrate dogs are depressed by μ and δ-opioids when applied directly to neurons in millimolar concentrations. However, a depression of these neurons of similar magnitude (50%) by intravenous remifentanil, a short-acting, potent, selective MOR agonist used for clinical analgesia, which leads to effect site (brain) agonist concentrations in the nanomolar range, could not be reversed by picoejection of the opioid antagonist naloxone directly onto the neurons. Thus we concluded that the μ-opioid effects occurred at sites upstream (presynaptic) from the respiratory premotor neurons. Because it has been shown that preBötC respiratory neurons supply synaptic inputs to the premotor neurons, we hypothesized that clinically relevant opioid-induced effects may be mediated via MORs on preBötC neurons.

2. RATIONALE, OBJECTIVES AND HYPOTHESIS

The rationale of the study is:

an understanding of where and how systemic opioids induce their effects on breathing patterns is the first step toward pinpointing the mechanisms underlying their depressive effects.

The objectives of this study are:

a) to determine whether systemic opioid induced depression of respiratory rhythm is produced by direct effects on MORs into the pre-BötC,
b) to determine whether is possible to reverse bradypnea caused by IV infusion of a MOR agonist with microinjection of MORs antagonist directly on respiratory neurons in the pre-BötC.

The hypothesis is that:

μ-opioid receptors on respiratory neurons in the pre-BötC are responsible for the bradypnea induced by μ-opioid receptor agonists.

3. METHODS

This study was approved by the subcommittee on animal studies of the Zablocki Veterans' Affairs Medical Center, Milwaukee, WI, in accordance with provisions of the Animal Welfare Act, the PHS Guide for the Care and Use of Laboratory Animals, and the institutional policy. Experiments were performed on Beagle dogs of either sex, weighing from 8 to 16 kg. Inhalational anesthesia was induced by mask and maintained with isoflurane (Abbott, Chicago, IL, SAD) at 1.5-2.5% end-tidal concentration. The animals were monitored for signs of inadequate anesthesia such as salivation, lacrimation, and increase in blood pressures and heart rate. If required, anesthetic depth was increased immediately.

3.1. Surgical procedures

The trachea of dogs was intubated with a cuffed endotracheal tube, and their lungs were mechanically ventilated with an air-O_2-isoflurane mixture. End-tidal CO_2 concentration was continuously recorded with an infrared analyzer (POET II, Criticare Systems Waukesha, WI, USA). A triple-lumen catheter was placed in the femoral vein and used for continuous infusion of maintenance fluids (0.9% NaCl) as well as drugs. The femoral arteries were cannulated for arterial blood sampling and continuous blood pressure monitoring (Gould-Statham P23 ID transducer, Oxnard, CA, USA). Blood gas samples were obtained periodically, and additional sodium bicarbonate was given to correct metabolic acidosis, if required. Esophageal temperature was monitored and maintained at 37.5-38.5ºC with a servo-controlled heating pad.

The dogs were positioned in a Kopf (model 1530 David Kopf Instruments, Tujunga, CA, USA) stereotaxic apparatus with the head flexed ventrally by 30º. The vertebral column was maintained straight through caudal tension applied via a hip-pin clamp. The right C5 phrenic nerve rootlet was exposed via a dorsolateral neck dissection, cut distally, desheathed, and placed on bipolar platinum electrodes in a mineral oil pool formed from a neck pouch. Phrenic nerve activity was recorded from desheathed right C5 rootlet. The phrenic neurogram (PNG) was obtained from the moving-time average (100 ms) of the amplified phrenic nerve activity and was used to produce timing pulses corresponding to the beginning and the end of the inspiratory phase for the measurement of inspiratory duration (T_I) and expiratory duration (T_E). Peak phrenic activity (PPA) was also obtained from the PNG.

To minimize brain stem movements during neuronal unit recording and feedback from extravagal afferents, a bilateral pneumothorax was created, and the animal was paralyzed with a 0.1 mg/kg i.v. bolus of pancuronium bromide (Hospira Inc., Lake Forest, IL, SAD) and supplemental doses of 0.05 mg/kg, as required. Bilateral cervical vagotomies were performed to eliminate afferent vagal input from pulmonary stretch receptors.

After a midline skin incision was made from the spinous process of the axis to the nasion, the muscles and underlying connective tissue were cut along the external sagittal and nuchal crests, dissected bilaterally, and reflected to expose the parietal bones from the midline to 4 cm laterally and from the nuchal crests to 4.5 cm rostrally. A high-speed drill with burr was used to drill the margins of exposed parietal bones to from 3.5-cm-long x 3.5-cm-wide bilateral craniotomy windows. These windows were placed ~0.5 cm lateral from the sagittal crest and ~1.0 cm rostral from the nuchal crest to avoid disruption of the dorsal sagittal and transverse venous sinuses.

Bone wax was applied to the cut bony edges to stop bleeding and to prevent potential air embolism. The dura was removed with scissors to expose the parietal and occipital lobes bilaterally. A bipolar coagulator (model 0441010; Burton Division of Cavitron Corporation, Van Nuys, CA, USA) with insulated, bayonet forceps (90-mm shaft, 2-mm tips; Edward Weck & Company, Research Triangle Park, NC, USA) was used to coagulate small volumes of brain tissue. With the sequential coagulation and suctioning of small amounts of the brain tissue, the caudal portions of the parietal and temporal lobes and the occipital lobe were removed bilaterally to expose the midbrain region. Cotton-tipped applicators were used for blunt dissection of midline brain structures under the falx and above the brain stem to expose the great cerebral vein and its main branches.

The vein was occluded with two metal clips and then transected to avoid accidental tearing, which could lead to air embolism. The applicators were also used to identify the midcollicular line, which runs just in front of the vermis and the commissure of the inferior colliculi. The origins of the oculomotor nerves were identified bilaterally on the ventral surface of the rostral mesencephalon by using the applicator to gently elevate (2-3 mm) the brain stem.

To facilitate brain stem transsection in the desired plane, the edge of spatula was placed by the side of the brainstem, from just behind the origin of oculomotor nerve ventrally and tilted toward the midcollicular line dorsally, to serve as a guide for the scalpel. The last few millimeters of the ventral brain stem were cut gently to avoid damage to the cavernous sinuses. In the case of bleeding, bleeding was stopped by gentle bipolar coagulation and with an absorbable hemostatic material, oxidized regenerated cellulose (Surgicel, Johnson & Johnson Medical, New Brunswick, NJ, USA).

After the decerebration procedure was completed. Isoflurane was gradually discontinued. An occipital craniotomy was performed, and the dura mater was opened along the midline and reflected laterally to expose the dorsal surface of the medulla oblongata (Figure 1).

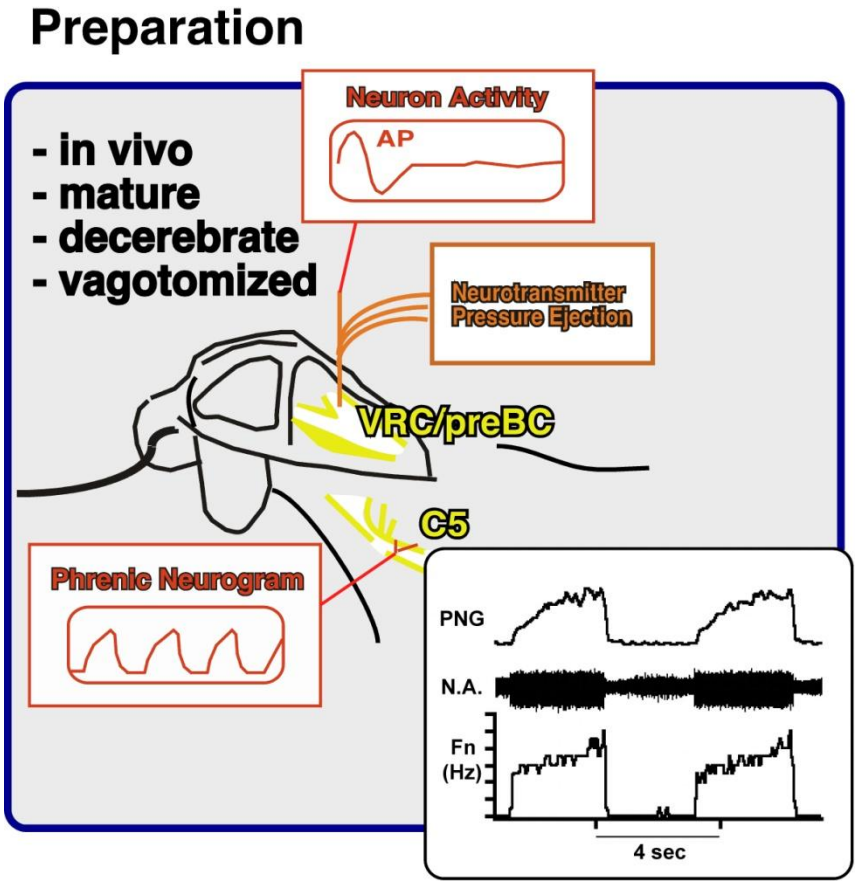

Figure 1. Decerebrate dog preparation. The phrenic neurogram was used to monitor changes in central inspiratory activity that result from IV infusion of MOR agonist and pressure

microinjections of the glutamate agonist (DLH), the MOR agonist or the opioid antagonist (NAL) into the pre-BötC.

3.2. Microinjection technique

A minimum of 1 hour was allowed for preparation stabilization before data collection. Extracellular neuronal recordings were obtained using multibarrel micropipettes (10-30 µm composite tip diameter) consisting of a recording barrel containing a 7 µm thick carbon filament and three drug barrels. The micropipettes were used to record pre-BötC respiratory neuronal activity within the ventrolateral medulla to verify the exact location of the ventral respiratory column (VRC) prior to pressure microinjections of the glutamate agonist D-homocysteic acid (DLH, 1 Mm, Sigma Aldrich, St. Louis, MO, USA) and the MOR antagonist naloxone (NAL, 500 µM and 5 mM, Abbott, Chicago, IL, USA) or the MOR agonist [$_{D}$-Ala^{2}, N-Me-Phe^{4}, Gly-ol^{5}]-enkephalin (DAMGO, 100 µM, Sigma Aldrich, St. Louis, MO, USA), which were dissolved in artificial cerebrospinal fluid (aCSF). Microinjections were made using an in-house, custom-built, four-channel microinjection system, which allowed independent control of ejection duration, repetition rate, and pressure (0-552 kPa). The microinjected drug volumes were measured via height changes of the meniscus in the pipette barrel with a 100X magnification microscope equipped with a reticule (resolution: ~2 nl).

3.3. Method for locating the preBötC region

Three criteria were used to locate the preBötC region: predetermined stereotaxic coordinates, presence of a mixture of respiratory neuron subtypes within the VRC, and PNG tachypneic response to DLH microinjections (30-40 nl; 20 mM, Figure 2). Previous studies showed that the canine preBötC can be found within a region in the VRC extending from ~3 to ~6 mm rostral to the obex. The region where the largest DLH-induced rate altering responses were observed consisted of a heterogenous mixture of propriobulbar I and E neuron subpopulations, which is consistent with observations in other species (44-46). The tachypneic response produced by DLH microinjection into the VRC has been accepted by many investigators as a functional marker of the preBötC region (37,38,44,47-49), and is the reason we used it in this study as one of the main criteria.

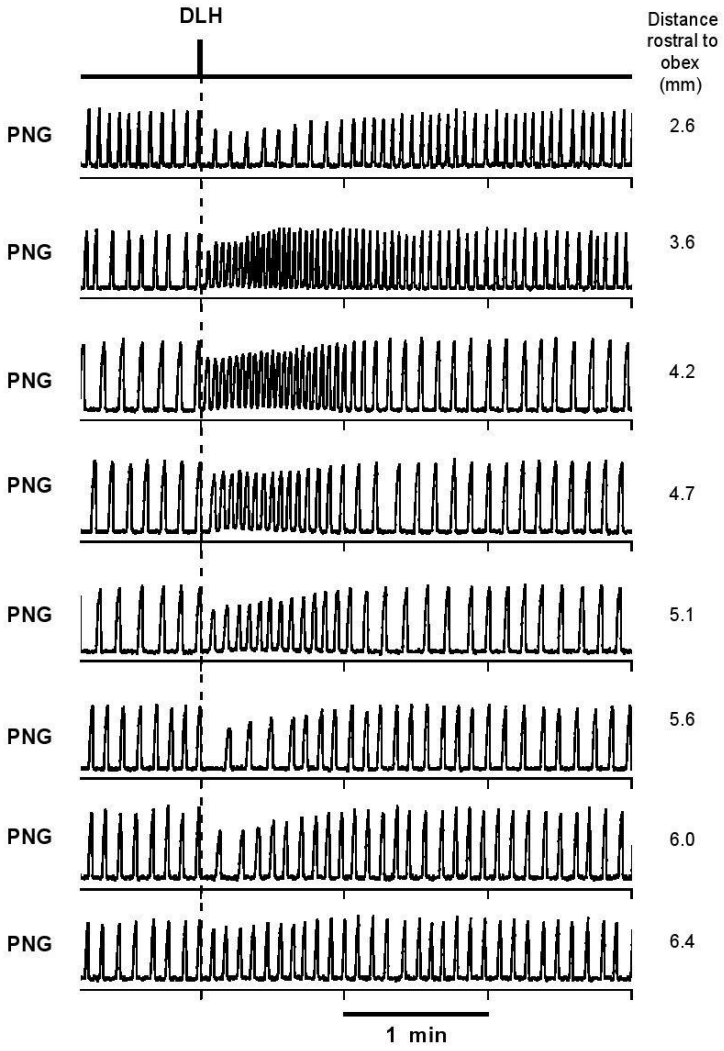

Figure 2. A series of DLH (20 mM) microinjections in the caudal-rostral direction within the canine ventral respiratory column of neurons was used to locate the maximum tachypneic response observed in the phrenic neurogram (PNG). This response functionally identifies the PreBöC at ~3.5-4.5 mm rostral to obex in this dog.

For the present study, starting at 3 mm rostral to obex and typically 4.5 mm lateral to the midline, the micropipette was advanced into the VRC, and the subtypes of neurons were noted from the dorsal to the ventral aspects of the VRC. The pipette was withdrawn to the midpoint,

and DLH was then microinjected while monitoring the PNG response. The micropipette was then removed, the tip cleaned, and then reinserted 1 mm more rostral, and the procedure was repeated, continuing to 7 mm rostral. The site within this region of the VRC with the maximum tachypneic response to DLH microinjection (~30 nl) was considered to represent the preBötC region (37). If no tachypneic response was found within the VRC, then coordinates and neuron subtype composition were used to locate the preBötC region.

3.4. Remi infusion

Remifentanil (Abbott, Chicago, IL, USA), (remi) is a pure μ-agonist analgesic drug whose effects are antagonized by naloxone. The analgesic effect is mediated through coupling of a guanine nucleotide binding protein (G protein) which concomitantly results presynaptically in an inhibition of excitatory neurotransmitter release and postsynaptically in an inhibition of cyclic adenosine monophosphatase, suppression of voltage-sensitive calcium channels, and hyperpolariztion of the postsynaptic membrane through increased potassium conductance. The range of clinically useful concentrations in anaesthesia is ~1-20 ng/ml (50).

The distinct advantages of using remi are its rapid onset and short latency to peak effect as well as its rapid recovery, which is independent of dose rate and length of infusion (Figure 3). These properties are due to remi's rapid metabolism by nonspecific esterases in the blood and tissues. Because it is short acting, remi must be continuously infused, and the infusion rate can be adjusted to produce steady-state responses of various degrees. The context-sensitive half-life, the time to a 50% decrease of an effective site concentration after infusion is stopped, has been estimated to be ~4 min for remi and is independent of infusion duration (51). The effective dose, which reduces minimum alveolar concentration of volatile anesthetics by 50% to surgical stimuli in humans, was found to be ~0.5 μg/kg/min and appears to be similar in dogs (52,53).

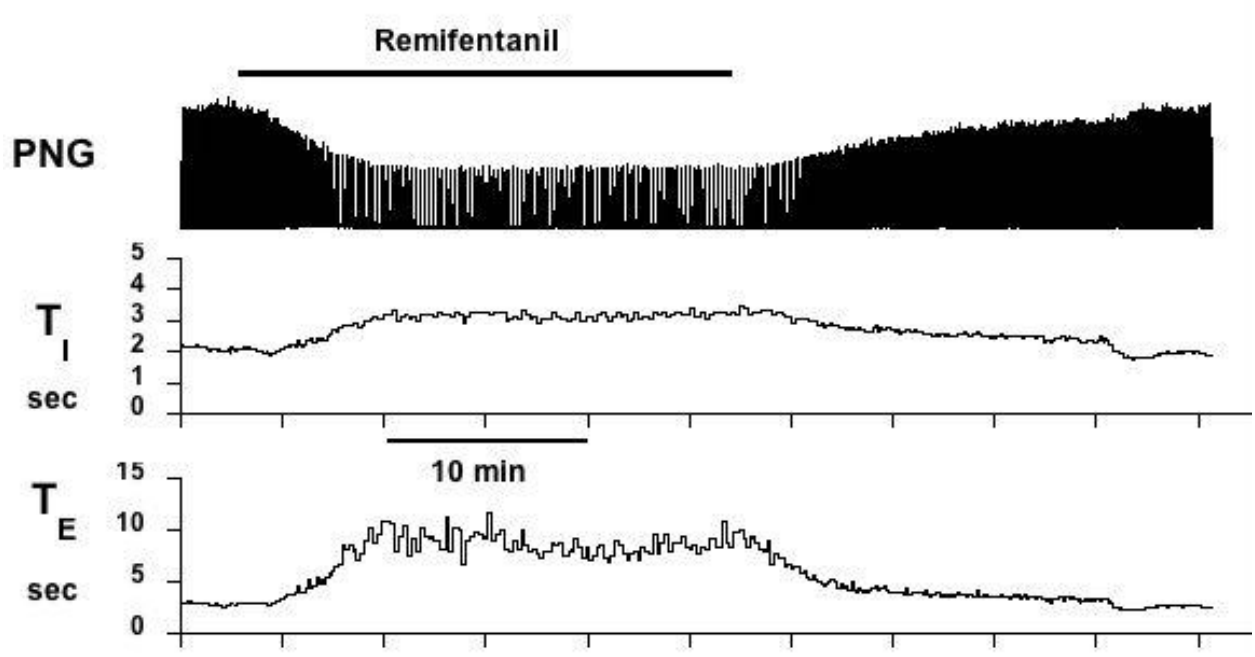

Figure 3. An example of remi induced bradypnea. Remi infusion (horizontal bar) produced an increase in inspiratory duration (T_I) and expiratory duration (T_E) and, in this case, a decrease in the peak phrenic neurogram (PNG).

3.5. Injection protocols

Protocol 1: Bilateral microinjection of NAL into the pre-BötC during intravenous remi-induced bradypnea.

After establishing a stable PNG baseline pattern, the preBötC region was located as previously described. Subsequently, remi was infused at an intravenous rate (~0.1-1.0 µg/kg/min) that resulted in a marked steady-state bradypnea (~60% decrease in central breathing frequency, f_B). During continued steady-state remi infusion, a series of bilateral injections of NAL (500 µM solution, ~120nl each), three on each side, centered in the preBötC and 1 mm rostral and caudal, were performed to locally block MORs. T_I, T_E, and PPA were continuously monitored on-line with a PowerLab system (ADInstruments, Castle Hill, Australia, 16SP and Chart

v5.5.6). Average values of these variables and f_B were obtained for off-line analysis before remi infusion and from data one min before and after each NAL microinjection during remi infusion. The same concentration (500 µM) NAL solution was finally given intravenously (total dose: ~60 µg/kg/iv) following completion of all direct preBötC NAL microinjections to verify its continued effectiveness in reversing the intravenous remi effects.

Protocol 2: Microinjection of DAMGO into the preBötC region: assessment of the direct MOR agonist effect on the phrenic nerve activity and breathing pattern.

After locating the preBötC region in the VRC in a separate second set of animals, DAMGO (100 µM) was microinjected into the preBötC region, and effects on the PNG were measured. After completion of the DAMGO microinjections, once maximal DAMGO effects on the PNG were observed, remi was infused intravenously to measure additional changes in the PNG that would have resulted from the systemic opioid effects on areas other than the preBötC. Then the remi infusion was stopped, and recovery from the remi-induced changes in f_B was awaited. Because the effects of preBötC DAMGO microinjections are long-lasting and outlast the effects of i.v. remi, the phrenic tachypnea reoccurred. This persistent DAMGO effect was then reversed by microinjection of a concentrated solution of NAL (5mM) into the same site (pre-BötC). To confirm that all DAMGO effects were limited to the preBötC region, this was followed, 10-15 min later, by intravenous NAL (~60 µg/kg), which would have antagonized any additional opioid effects on the brainstem. In a subset of four dogs, DAMGO was injected bilaterally into the preBötC to measure any additional direct effects.

Protocol 3: Picoejection of NAL onto single preBötC neurons during remi-induced bradypnea.

After locating the preBötC region in the VRC in a separate third set of animals, control recordings were made before and during remi-induced bradypnea. During steady-state bradypnea, when preBötC neuronal discharge frequencies are typically depressed by 25-50%, NAL (500 µM) was continuously picoejected onto the depressed neuron at increasing picoejection rates up to a level, which was estimated to approach the barrel concentration. Subsequently, the intravenous remi infusion was stopped, and the neuronal activity was

monitored during the recovery phase from remi. The micropipette was then repositioned in a new location ≥500 μm distant from the previous track to avoid contamination from residual effects of intramedullary NAL, and the protocol was then repeated. In addition, at least once per animal, picoejection of the aCSF vehicle was used to verify that the aCSF constituents and ejected volumes were without effect on single neurons. A time-amplitude window discriminator was used to generate a standard logic pulse for each spike. Neuronal discharge frequency, F_n, was continuously determined on-line by the number of discharges in each 100-ms time increment. Neuronal and phrenic activity and the picoejection marker signals were recorded on a digital tape system (Model 3000A, A. R. Vetter, Rebersburg, PA, USA) for further off-line analyses. Cycle-triggered histograms (CTHs; 50-ms bins) of the tape-recorded neuronal discharge were generated from template-discriminated spikes (Spike2, v6.04, Cambridge Electronic Design, Cambridge, UK). Peak and average discharge frequency were determined from the CTHs (15-20 cycles/CTH) and used to measure the remi and NAL effects.

3.6. Data analysis

Statistical procedures were carried out using SigmaStat 3.5 (Systat Softaware, Richmond, CA, USA). A one-way repeated-measures ANOVA was used on data that were normalized relative to control values. A general linear model was automatically used to provide least-squares estimates of the means for cells with missing data and unbalanced data sets. The Holm-Sidak method was used for pairwise multiple comparisons with a family-wide error rate of 0.05. For all data sets, tests for normality of the normalized data (Kolmogorov-Smirnov test) were performed before parametric procedures were used. For data sets that failed the normality test, a Kruskal-Wallis one-way ANOVA on ranks was used with Dunn's method for pairwise multiple comparisons. Differences were considered significant for $P < 0.05$. Values are expressed as mean ± standard error (M ± SE).

4. RESULTS

We found that the tachypneic region associated with the canine preBötC region was located within the VRC at 4.3-6.8 mm rostral to obex, 4-5 mm lateral to the midline and 6-8 mm below the dorsal medullary surface. The area also contained a mixture of inspiratory and expiratory neuron subpopulations as have been previously shown by Krolo et al (37).

Protocol 1. Bilateral microinjections of Naloxone into the preBötC during intravenous remi-induced bradypnea

An example of this protocol is shown in Figure 4, which shows traces of the PNG, injection markers, and breathing rate f_B. The DLH microinjection produced a strong tachypnea (from 12 to 30 breath/min; BPM), indicative of the preBötC region. Intravenous infusion of remi (0.22 µg/kg/min) decreased f_B to ~5 BPM. During steady-state remi-induced bradypnea, a series of NAL microinjections (120 nL each) were made on the right side and then the left side of the medulla centered in preBötC region. Microinjections were placed at the center of the maximum tachypneic region and 1 mm rostral and 1 mm caudal to it. At each site two microinjections were made separated by ~0.5 mm in depth. Note that none of the local NAL microinjections had any effect on f_B (Figure 4 C & D). In Figure D, augmented PNGs or sigh-like activity is apparent. Such sighs may be seen at baseline and can become more frequent during intravenous remi-induced bradypnea in some, but not all dogs, with and without NAL microinjections.

In contrast to preBötC NAL microinjections, intravenous NAL rapidly reversed the remi-induced bradypnea and depression of phrenic amplitude. This reversal tended to transiently overshoot beyond the control baseline levels to varying degrees (Figure 4*E* and 5, NAL IV bars). A transient intravenous NAL-induced overshoot was also regularly seen in systemic blood pressure (data not shown). Note that due to a very gradual increase in the central respiratory rate over time (which is typical in this type of preparation) despite steady-state intravenous remi, f_B had increased prior to the IV NAL injection (Figure 4E) and was much higher afterward relative to the initial baseline rate (Figure 4A). A slow, spontaneous increase in breathing frequency can be often seen in decerebrate dogs without, as well as during steady-

state remi infusions, but such slow increase occur over many hours so that they do not influence or negate assessment of the effects of interventions over shorter time spans (e.g., <30 min).

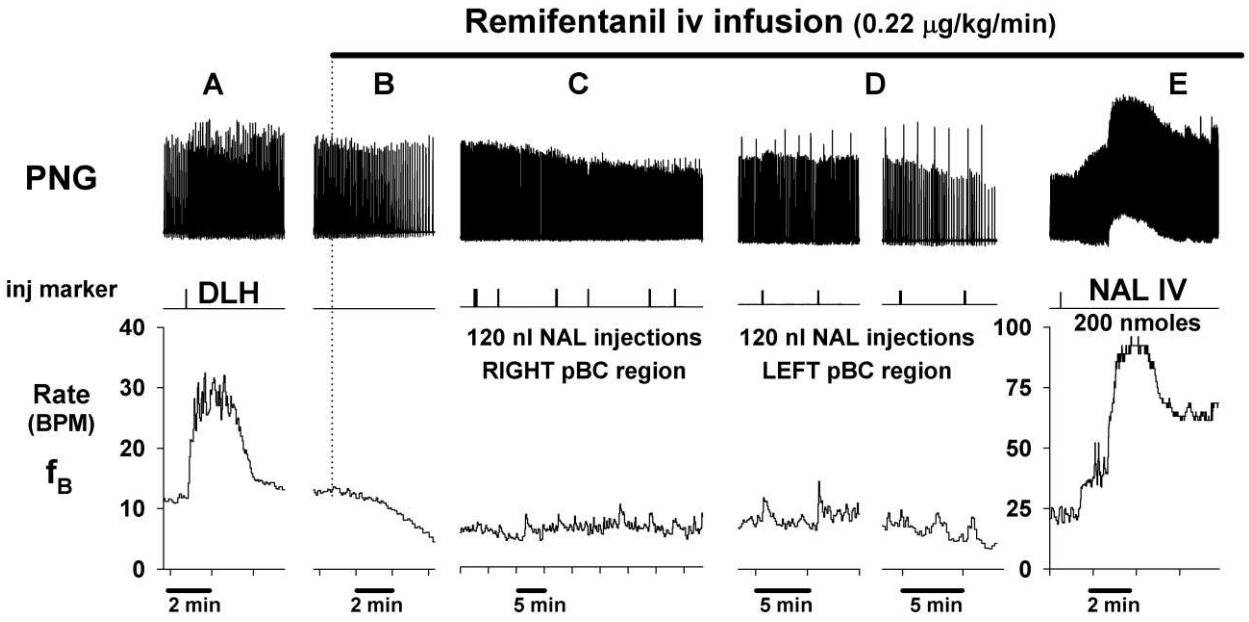

Figure 4. Example of protocol 1: bilateral microinjections of naloxone into the preBötC region fail to antagonize intravenous remifentanil-induced bradypnea: *Top:* phrenic neurogram (PNG); *middle:* microinjection marker; *bottom:* phrenic burst rate or fictive breathing rate. A: D-homocysteic acid (DLH) microinjection induces tachypnea, which functionally identifies the preBötC location. *B*: intravenous remifentanil infusion (upper horizolntal bar) produces a gradual reduction in phrenic burst rate. *C* and *D:* during steady-state IV remi-induced bradypnea, multiple microinjections of naloxone (NAL) into area of preBötC (pBC) in the right and left ventral respiratory columns fail to antagonize IV remi-induced bradypnea. Of note, remi can cause occasional sighs as visible in *D*. *E*: intravenous NAL (NAL IV) promptly reversed the remi-induced bradypnea with an overshoot tachypnea.

In 15 dogs, remi (0.50 ± 0.13 µg/kg/min) decreased f_B by 41 ± 7% from 27.5 ± 4.6 to 14.5 ± 3.6 BPM, decreased PPA by 32 ± 3%, decreased neural minute ventilation by 60 ± 6% (Figure 5, left), increased T_I by 17 ± 4%, and increased T_E by 143 ± 14% (Figure 5, right).

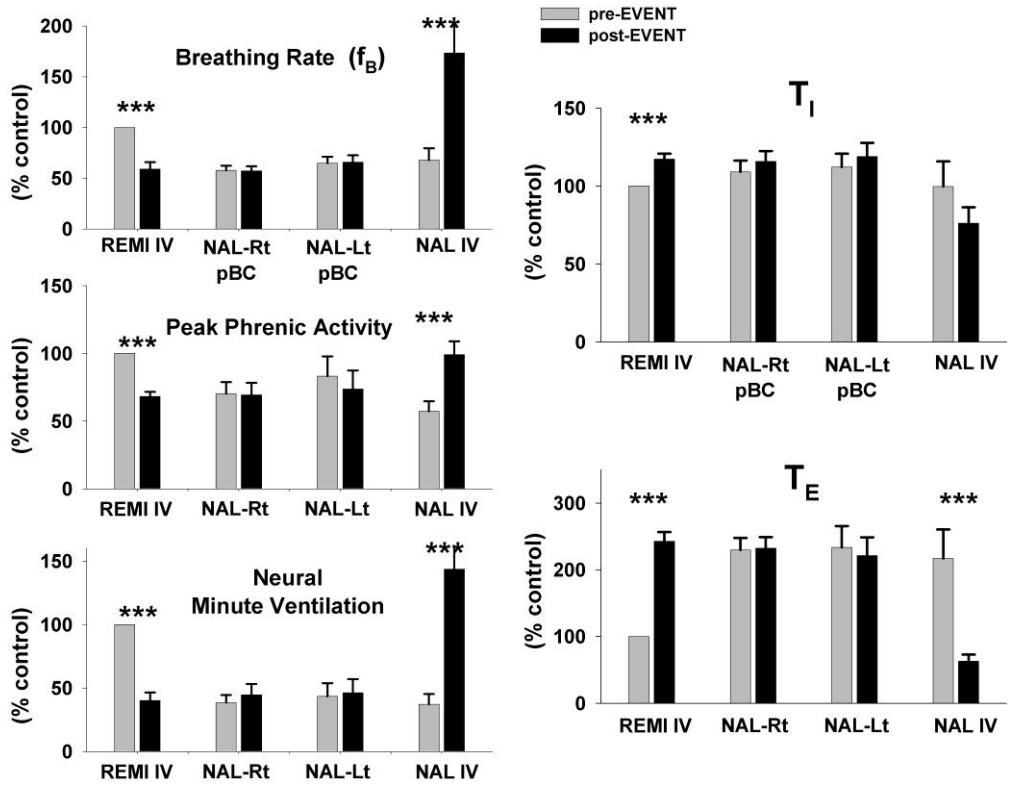

Figure 5. Summary data for protocol 1 from 15 dogs confirm that right-sided (Rt) and left-sided (Lt) microinjections of NAL into pre-BötC failed to reverse the intravenous remi-induced bradypnea (REMI IV), while intravenous NAL (NAL IV) promptly reverses the remi effects with overshoot tachypnea. *Top left:* phrenic (burst) breathing rate; *middle left*: peak phrenic activity; and *bottom left*: neural minute ventilation (f_B x PPA). *Right*: intravenous remi (REMI IV) induced a modest prolongation of inspiratory duration (T_I) and marked prolongation of expiratory duration (T_E), but bilateral microinjections of NAL into the preBötC failed to have any effect (NAL-Rt pBC; NAL-Lt pBC), whereas intravenous NAL (NAL IV) promptly reversed the remi effects. All values are normalized to control values, see text for details. ***, $P < 0.001$ for significant differences between pre-events (□) and post-events (■).

An average protocol took 2.6 h to complete. The time from the start of the remi infusion to the first NAL injection was 55 ± 10 min (Figure 6, Remi-R1), and the average time between injection sites was 16 ± 2 min (Figure 6, average of middle 5 bars), which included cleaning the micropipette tip, insertion in the new location, locating neuronal activity in the VRC, placing two injections of ~125 nL each (Figure 7, upper) and ~0.5 mm apart in the dorsal and ventral regions of the VRC, and micropipette withdrawal.

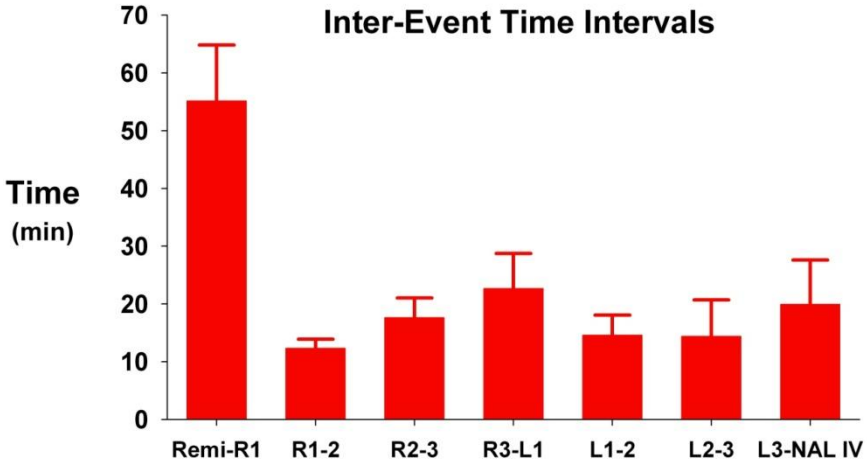

Figure 6. Summary of time intervals between events. The 1st NAL microinjection was given ~55 min. after the start of the remi infusion. Time between site-to-site injections ranged from 10-20 min. (required to localize VRC neuronal activity prior to microinjection). Total protocol time averaged ~3 hrs.

Based on a brain extracellular volume fraction of 0.21 [fraction of the total brain tissue volume (54)], each 125 nL injection volume would have a spherical diameter of ~1 mm (Figure 7, lower, estimated diameters) and with subsequent diffusion would have an even larger effective volume diameter. Thus three injections that are 1 mm apart would allow the effects of NAL to extend over 3 mm in the rostral-caudal direction of VRC preBötC region and well over 1 mm in the other directions. Despite the relative large projected volume of spread, Figure 5 shows that

the NAL microinjections had no effect on any of the phrenic respiratory timing and drive variables.

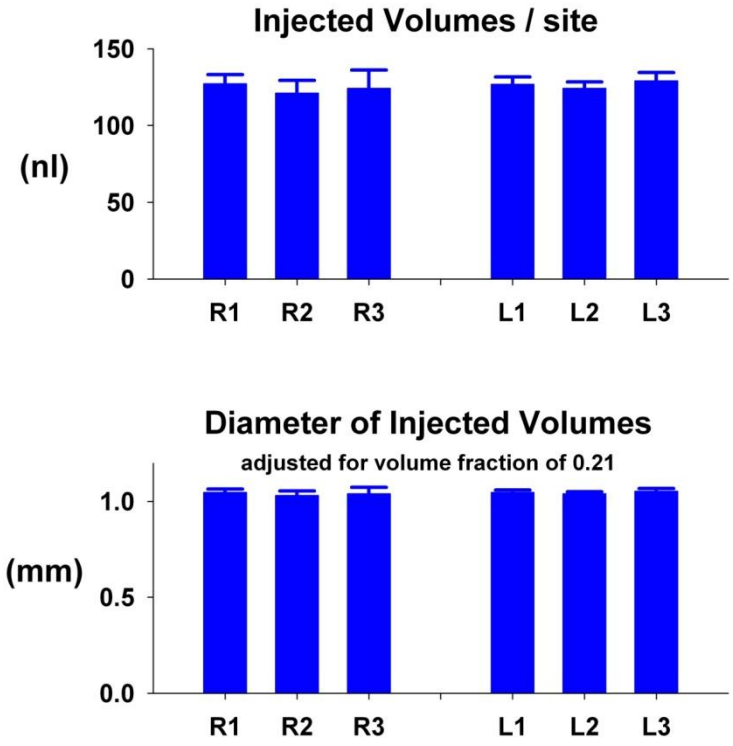

Figure 7. Summary of injected volumes at each site. Upper: Two ~120 nL injection were made per site. Lower: Estimated diameter of each injection (~1 mm) based on spherical geometry and adjusted for 21% extracellular volume.

To correct for the effect of time drift on respiratory rate from the onset of the protocol, changes in the variables were always analyzed relative to their immediate local control values, that is, the value preceding each injection. As shown in Figure 8 with such corrections, there were no changes in PPA, T_I, and T_E following the NAL injections. In stark contrast, intravenous NAL (60.7 ± 19 µg/kg) during the remi infusion promptly and fully reversed the remi-induced effects (Figure 5, NAL IV).

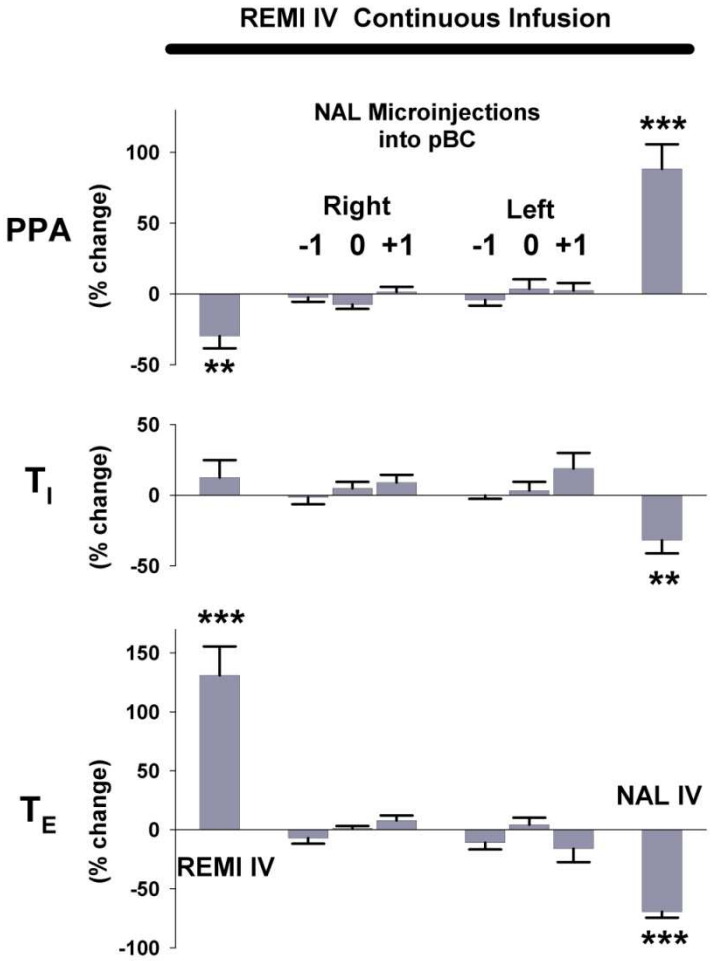

Figure 8. Summary data for protocol 1 shown as changes relative to their immediate local control values to minimize the slow drift in variables over the long protocol. These data for 15 dogs confirm that the right and left-sided microinjections of NAL into the preBötC (pBC) region failed to reverse the intravenous remi (REMI IV) induced depression of phrenic amplitude (PPA) and the prolongation of T_I and T_E, while intravenous NAL (NAL IV) promptly reversed all REMI IV effects (e.g., seen in Figure 4). **, $P < 0.01$; ***, $P < 0.001$ for significant differences from no change.

Protocol 2. Microinjection of DAMGO into the pre-BötC region: assessment of the direct MOR agonist effect on the phrenic nerve activity

Figure 9 shows an example of the protocol used to study the effects of microinjection of the MOR agonist DAMGO into the preBötC region on the PNG pattern.

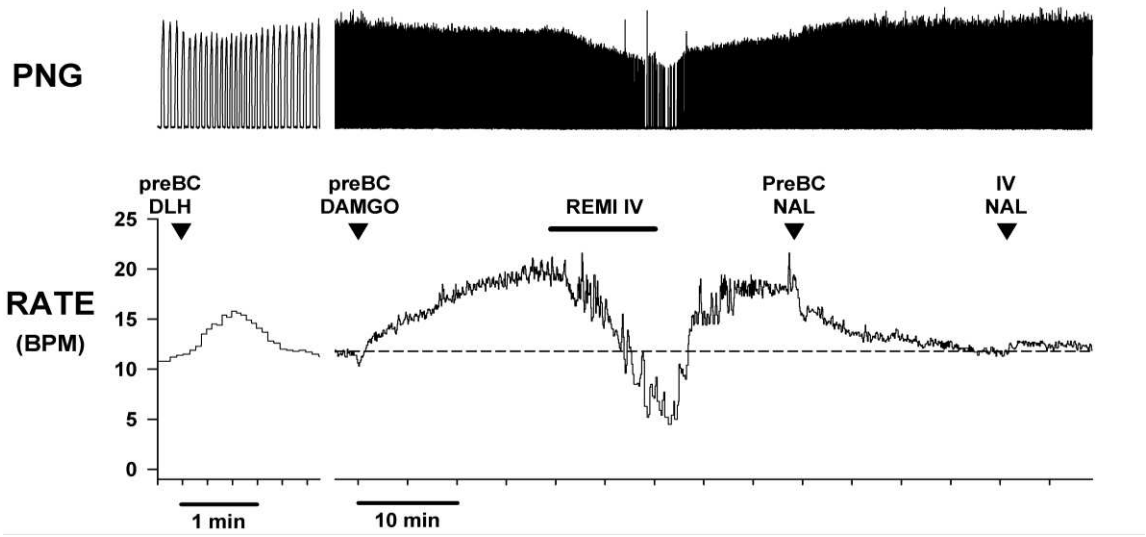

Figure 9. Example of a protocol 2 run shows that microinjections of DAMGO into the preBötC region increased the phrenic burst rate. *Top:* the PNG and bottom: the fictive respiratory rate derived from the phrenic neurogram. From left to right: DLH microinjection (44 nl: 20 mM) induces tachypnea, which locates preBötC. Subsequent unilateral microinjection of DAMGO (109 nl: 100 µM) at the same site increased respiratory rate with only minor effects on peak phrenic activity. Intravenous remi (REMI IV; 0.8 µg/kg/min) overcame the effects of DAMGO and, on the contrary, produced a profound bradypnea and depression of peak phrenic activity. Following the recovery from remi of respiratory rate and peak phrenic activity, microinjection of NAL (360 nl; 5 mM) into the same site where DAMGO was microinjected, gradually reversed the DAMGO-induced tachypnea. Subsequent intravenous NAL (NAL IV; 79 µg/kg) produced little or no additional effect.

The preBötC region was functionally identified within the VRC, where I and E neurons were found, by the typical tachypneic response produced by DLH microinjection (Figure 9, left, preBC DLH). Following recovery of the response to DLH, 109 nL of 100 µM DAMGO was microinjected into the same site, and f_B increased from ~12 to ~20 BPM (67%increase) over a 15 min period. In contrast, the intravenous infusion of 0.8 µg/kg/min remi, after the maximal DAMGO effect was reached, produced a pronounced decrease in f_B to ~5 BPM (Figure 9, REMI IV bar). After recovery from the remi-induced bradypneic effects (~10 min), the prolonged residual DAMGO effect caused a return to relative tachypnea. At this point, microinjection of NAL (360 nL; 5 mM) into the same site, where DAMGO was microinjected, gradually reversed the DAMGO-induced tachypnea with the return of respiratory rate to pre DAMGO baseline (Figure 9, PreBC NAL, dashed horizontal line). Subsequent intravenous NAL (NAL IV; 79 µg/kg) produced no additional effect in this animal. Typically DAMGO-induced effects lasted >1 h before spontaneous resolution. The overall protocol took ~90 min to complete.

The pooled data (n=16 dogs, Figure 10) show that unilateral microinjection of 100 µM DAMGO (143 ± 16 nL) into the right pre-BötC region increased f_B by 44 ± 5.2% from the baseline f_B of 17.7 ± 2.9 BPM. This was due to a 25 ± 3% decrease in T_I and a 35 ± 4% decrease in T_E (Fig. 10B), where baseline T_I and T_E values were 1.64 ± 0.20 and 3.35 ± 0.64 s, respectively. PPA was decreased by 12 ± 4%. Subsequent microinjection of NAL (211 ± 39 nL, 5 mM) at the same location as the DAMGO microinjections could only partially antagonize the DAMGO-induced tachypnea, reducing f_B to 25.7 ± 7.3% above control, but restored PPA to control levels (Figure 10A, NAL pBC). However, intravenous administration of NAL (76 ± 5 µg/kg iv) produced additional and nearly complete antagonism of the DAMGO effects in the preBötC region. In 4 of 16 dogs, bilateral DAMGO microinjections in the preBötC regions were studied to determine the magnitude of the additional DAMGO injection. The pooled data (Figure 10C, top) show that the right sided microinjections increased f_B from 14.5 ± 2.3 to 21.4 ± 4.3 BPM or ~48%. Additional left-sided DAMGO microinjections increased f_B to 24.6 BPM or a further 22%. Subsequent intravenous NAL returned f_B to control levels.

In 7 of the 16 dogs, remi (1.0 ± 0.1 µg/kg/min) was infused intravenously after the DAMGO microinjections, i.e., while the DAMGO effects persisted, to compare systemic versus local µ-

opioid effects on f_B. In this study, unilateral microinjection of DAMGO increased f_B by 51 ± 16%, whereas intravenous remi decreased f_B by 55 ± 8% relative to control (Figure 10C, bottom). Only after complete recovery from the remi effects, local NAL microinjections were given, followed by intravenous NAL injections.

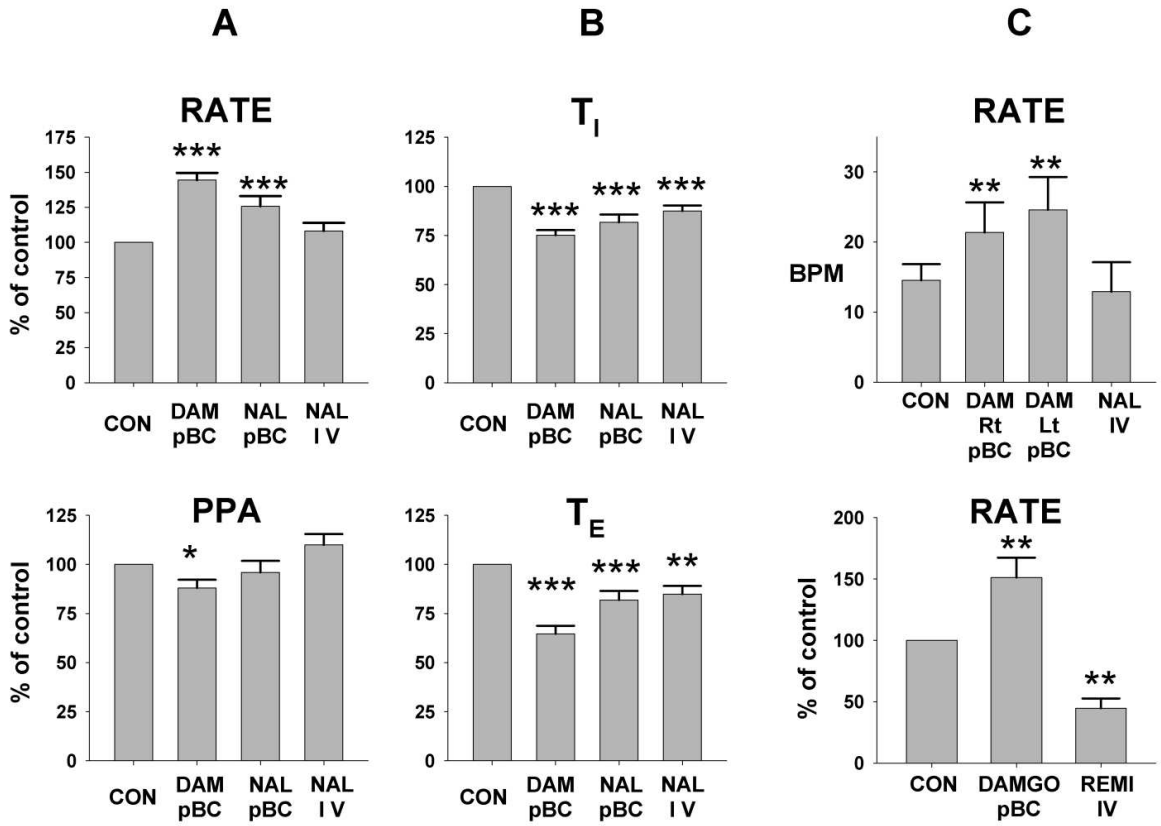

Figure 10. Summary of the normalized pooled data for protocol 2 (n = 16) shows that unilateral microinjection of DAMGO into the right preBötC region increased breathing rate (A, *top, 2nd bar,* DAM pBC). This was due to decrease in T_I (B, *top, 2nd bar,* DAM pBC) and T_E (*B*, *bottom, 2nd bar,* DAM pBC). PPA was only modestly decreased (A, *bottom, 2nd bar,* DAM pBC). Subsequent microinjection of NAL (NAL pBC) at the same location as the DAMGO microinjections only partially antagonized the DAMGO-induced tachypnea (A, *top, 3rd bar*) but restored PPA to control levels (A, *bottom, 3rd bar*). However, intravenous administration of NAL (NAL IV) produced complete antagonism of the DAMGO effects in the preBötC region. C, *top*: summary of the pooled data from 4 of the 16 dogs with sequential bilateral DAMGO microinjections in the preBötC region. Additional left-sided DAMGO (DAM Lt pBC)

microinjections increased phrenic respiratory rate further, but the difference from the right-sided unilateral DAMGO (DAM Rt pBC) microinjections was not statistically significant. Subsequent intravenous NAL (NAL IV) reversed the DAMGO effects and returned the rate to control levels. C, *bottom*: summary data from 7 of 16 dogs, in which remi (REMI IV) was infused intravenously after the DAMGO microinjections to compare systemic vs. local μ-opioid effects on phrenic respiratory rate. Unilateral microinjection of DAMGO (DAMGO pBC) increased respiratory rate, whereas intravenous remi (REMI IV) decreased the respiratory rate relative to control. The 2 effects acted in opposite directions. *, $P < 0.05$;**, $P < 0.01$; ***, $P < 0.001$ for significant differences from control.

Protocol 3. Picoinjection of NAL onto single neurons in or near the preBötC region during remi-induced bradypnea

Figure 11 shows an example of protocol 3 for an inspiratory decrementing neuron in or near the preBötC region. Intravenous infusion of remi (0.16 μg/kg/min) decreased the peak discharge frequency (F_n) from 32.2 to 20.2 Hz (~37%) and decreased the decrementing rate (Figure 11A). Picoejection of NAL (500 μM at 2.9 nl/min or 1.45 pmol/min) onto this neuron had no effect on reversing the remi-induced depression (Figure 11B), but the neuron's discharge pattern completely recovered following termination of the remi infusion (Figure 11C). The pooled data from three inspiratory and three expiratory neurons (Figure 12) indicate that highly localized application of NAL did not reverse the remi-induced depression of neuronal activity. Intravenous remi (0.20 ± 0.03 μg/kg/min) produced a 37.2 ± 9.8% decrease in peak F_n and a 29.8 ± 11.2% decrease in the time-averaged F_n (Figure 12, F_{peak} and F_{ave}).

Picoejection of NAL (4.4 ± 1.2 pmol/min) had no effect, but neuronal activity completely recovered following termination of remi infusion. Even though we found that none of six neurons (0/6) respond to NAL, with this small sample, it is possible to miss neurons depressed by remi that would have been reversed by local NAL. Without prior knowledge of the proportion of the neuron population that is unresponsive, a 95% confidence interval analysis suggest that the proportion of neurons that did not respond to NAL lies between 0 and 46% (55).

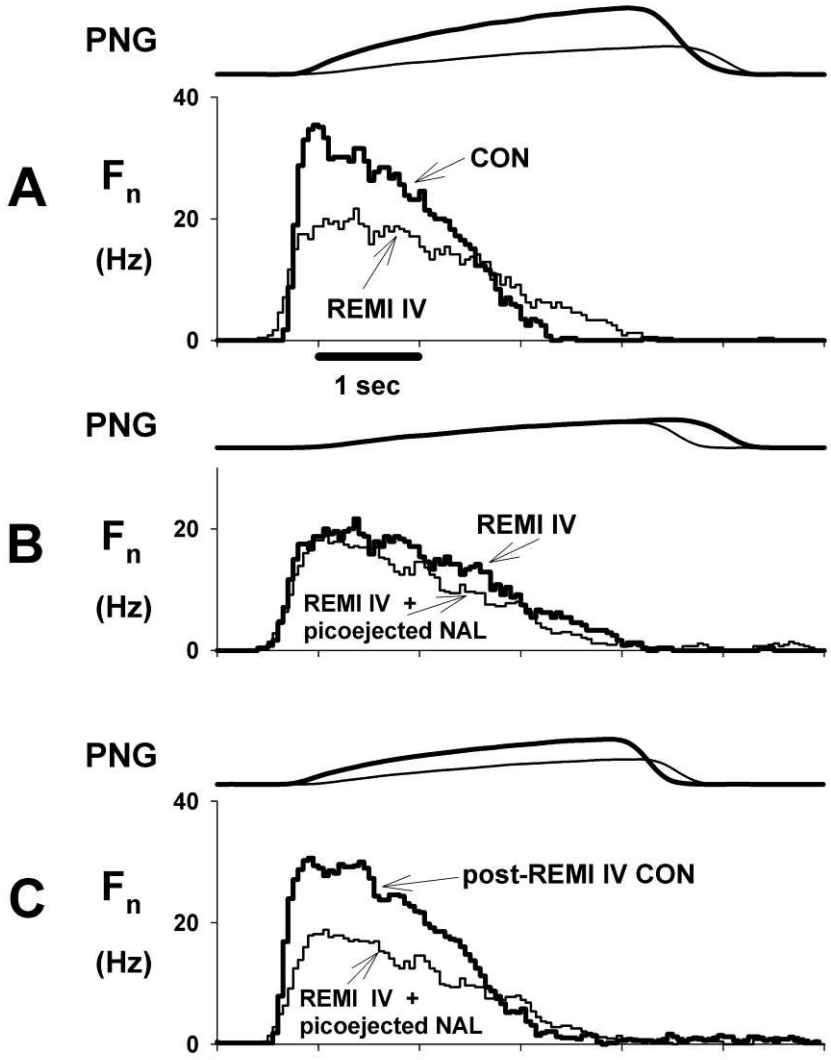

Figure 11. Example from an inspiratory preBötC neuron with a decrementing discharge pattern from protocol 3. *Top trace* of each panel shows effect on PNG; *bottom trace* of each panel shows effect on neuronal discharge pattern as a cycle triggered histogram of the discharge frequency. A: phrenic and neuronal activities were depressed by intravenous remi (REMI IV) from control (CON). *B*: picoejection of NAL (picoejected NAL) onto the neuron during remi-induced depression (REMI IV) did not reverse the decrease of the peak discharge frequency. *C*:

phrenic activity and neuronal discharge almost fully recovered after cessation of the intravenous remi infusion (post-REMI IV CON).

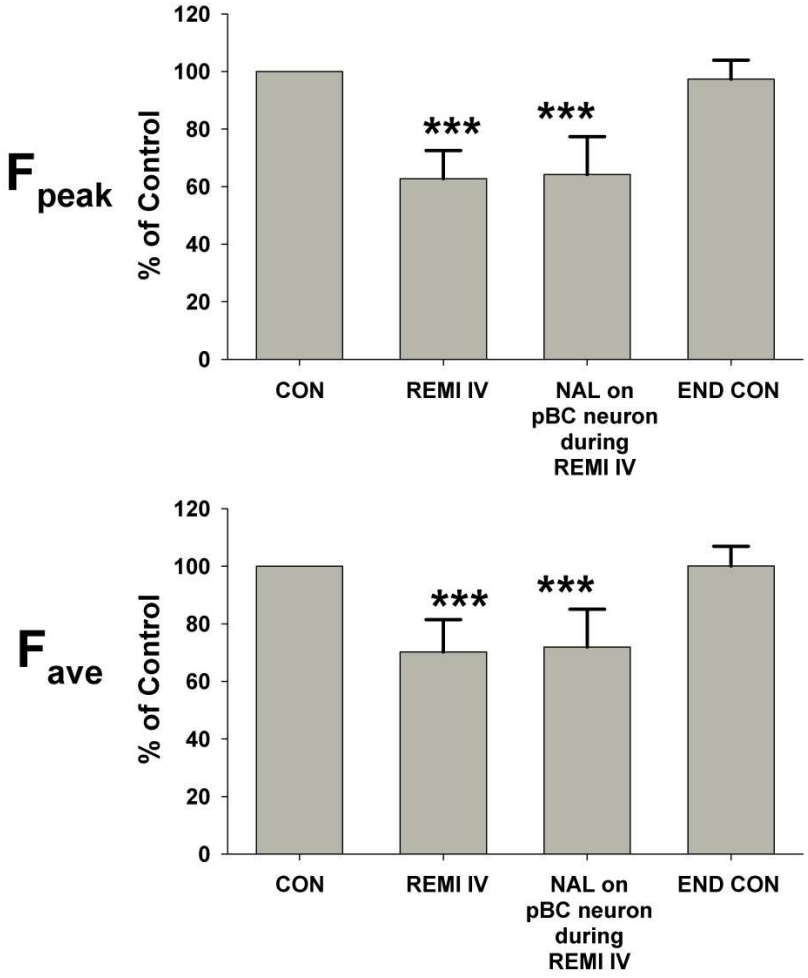

Figure 12. Pooled data for protocol 3 from 3 inspiratory and 3 expiratory neurons. *Second bar* of each panel show that intravenous remi infusion (REMI IV) decreased peak and time-averaged discharge frequency (F_{peak} and F_{ave}). Picoejection of NAL (NAL during REMI IV, 3rd bar) onto the neuron in the preBötC did not reverse the remi-induced depression of neuronal activity. Neuronal activity completely recovered following termination of remi infusion (END CON). ***, $P < 0.001$ for significant differences from control (100%).

The anatomical sites of the NAL and DAMGO microinjections and studied neurons, as determined by the stereotaxic coordinates relative to the obex, midline, and dorsal surface, are shown in Figure 13. The microinjection sites were always in a region of respiratory neuronal activity, presumably the VRC.

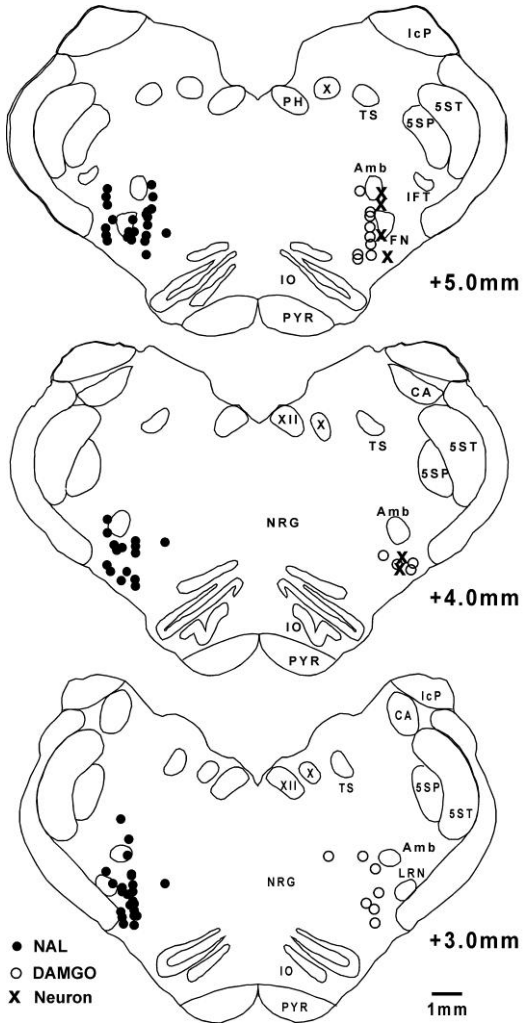

Figure 13. Coronal sections of the brainstem in the area of the preBotC show the anatomical sites of the NAL (□) and DAMGO (o) microinjections and neurons (x) relative to the obex, midline and dorsal surface. For clarity, NAL and DAMGO injections are shown on separate sides.

Acronyms:

Amb – nucleus ambigus; 5ST – tractus spinalis n. tigemini; PYR – tractus pyramidalis; CA – nucleus cuneatus accesorius; TS – tractus solitaries; NRG – nucleus reticularis gigantocelularis;

LRN – lateral reticular nucleus; X – nucleus dorsalis n. vagi; XII – nucleus n. hypoglossi; IO – inferior olivary nucleus; 5SP – nucleus spinalis n. trigemini; IcP – penduculus cerebellaris inferioris; PH – nucleus prepositus hypoglossi.

5. DISCUSSION

The main finding of this study is that the bradypnea produced by systemically administered μ-opioids at clinically relevant doses for analgesia is not caused by direct MOR activation in the preBötC. Rather, direct activation of preBötC MORs with the selective agonist DAMGO consistently produced tachypnea. This conclusion is also supported by the lack of a reversing effect of NAL on single preBötC neurons that were depressed during intravenous remi infusion, within the limits imposed by the small sample size (n=6). These findings suggest that MORs on neurons presynaptic to the preBötC must be responsible for the bradypneic response. In addition, although there are functional MORs in the preBötC, their in vivo role in the control of breathing is not clear. It is clear that high local opioid agonist concentrations in the micro-to millimolar range are required to directly depress respiratory neurons in the preBötC, similar to our findings for VRC premotor neurons (43). Such high concentrations may be reached by synaptic release of endomorphins, i.e., preBötC MORs may be synaptically activated by endogenous peptides (56,57). It is known from other neurotransmitters that their transient synaptic concentrations can reach the millimolar range (58,59).

In a minority of animals, mostly those with low baseline respiratory rates, an increase in respiratory rate with remi rather than a slowing was observed. These animals were not used for the study protocols. This discrepancy to the clinical experience with patients is likely due to our particular experimental setup. Vagotomy may eliminate a direct opioid effect on vagal inputs and thus reduce slowing. Also the increase in arterial CO_2 that results from opioid application in spontaneously breathing patients can cause slowing of the respiratory rate, whereas in our animals, ventilation was controlled and CO_2 remained unchanged.

In some dogs, remi infusion was associated with sigh-like PNG cycles. Sighs occur even in the absence of NAL microinjections, but seem to be induced by, or increased by remi. Currently it is not known where and how they are generated, although they have been reported to occur in brainstem slices that include the preBötC (60).

Methodological considerations

Three criteria were used to locate the preBötC region: predetermined stereotaxic coordinates, presence of a mixture of respiratory neuron subtypes within the VRC, and PNG tachypneic response to DLH micorinjections (30-40 nl; 20 mM). The preBötC region in the dog consists of a heterogenous mixture of propriobulbar inspiratory and expiratory neuron subpopulations and is located within the VRC at 4.3-6.8 mm rostral to obex (37). The region where the largest DLH-induced rate altering typically tachypneic responses were observed consisted of a heterogenous mixture of propriobulbar I and E neuron subpopulations, which is consistent with observations in other species (44-46).

The tachypneic response produced by DLH microinjection into the VRC has been accepted by many investigators as a functional marker of the preBötC region (37,38,44,48,49) and is the reason it was used in this study as one of the main criteria. In this study it was always made sure that the electrode tip was in the VRC by recording respiratory neuronal activity and furthermore, that the area within VRC, which we considered to be the preBötC, consisted of a mixture of various subtypes of I, E and phase-spanning neurons, which is a hallmark of the preBötC. Within this area, the preBötC was considered to be in the location that showed the most pronounced change in phrenic burst rate to a microinjected DLH.

It is possible to be fairly certain that the local microinjections were large enough to achieve a near maximal drug effect on most of the neurons of the preBötC. Based on a brain extracellular volume of 21%, each 125 nl injection volume theoretically would have a spherical diameter of ~1 mm and with subsequent diffusion would have an even larger effective volume diameter. For example, a 1 nl injection volume would produce a droplet with a spherical radius of 62 µm. The size and spread of multiple NAL injections (~125 nl, >3 mm in the rostral-caudal direction, centered at the point of maximum tachypnic response and >1 mm in the medial-lateral and dorsal-ventral aspects of the VRC) most likely exceeded the boundaries of the preBötC region. Microinjections were only made in the ventrolateral medulla where respiratory neuronal activity was found.

In addition, the concentration of microinjected NAL (500 µM) was >1,000 times greater than the plasma concentration that was required for reversal of remi-induced effects by intravenous

NAL. Furthermore, because diffusion occurs with NAL microinjections, the effective volume of MOR antagonism by local NAL would be much greater than the microinjected volume. Finally, microinjections of DAMGO into the same region induced a reproducible tachypneic response consistent with direct activation of MORs on neurons in the preBötC region. On the other hand, the fact that NAL microinjections did not have any effect on the PNG suggests that diffusion of the drug was limited to the VRC and did not affect other areas of respiratory control.

The conclusions are based on whole phrenic nerve recordings during micorinjections into a network of neurons; however, these conclusions are also supported at the cellular level. Picoejection of NAL on single preBötC neurons (n=6) failed to reverse any of the neuronal depression induced by intravenous remi. Similarly, a previous study found that none of the 18 (95% confidence interval: 0-18.5%) bulbospinal respiratory premotor neurons studied were affected by NAL picoejection during intravenous remi-induced depression even though these neurons have been shown to have μ- and δ-opioid receptors using selective agonists (43) .

A possible explanation for the lack of a direct effect on preBötC MORs by systemic administration of remi is the low plasma and thus brain concentration levels that are attained. The typical remi infusion rates that were used (~0.5 μg/kg/min) are expected to result in plasma concentrations of ~10 ng/ml or 24 nM in dogs (52), which is ~4,000 times less than the concentration of microinjected DAMGO (100 μM), which induced a tachypneic response. An IC_{50} of 35 ± 9 nM for DAMGO inhibition of cAMP production was found in cells expressing cloned MORs (61). In mice, the unbound brain EC_{50} concentrations for remi related opioids, fentanyl, alfentanil, and sulfentanil, have been found to be very similar to the unbound EC_{50} serum concentrations and to the in vitro affinity (K_i) (62). Because remi is about half as potent as fentanyl (53), the estimated affinity K_i for remi would be between 5 and 10 nM. This may explain why the targeted ~24 nM remi plasma concentration that was used in the current study induced the observed, marked bradypneic responses, assuming that highly opioid-sensitive sites responsible for respiratory rate control were affected.

In the previous study on VRC bulbospinal premotor neurons, where intravenous remi had only upstream effects but no direct depressant effects at the premotor neuronal level, picoejection of remi at concentrations >20 times larger than reported peak plasma concentrations had no effect

on the discharge of single neurons. A similar scenario may take place in the more rostral preBötC region. Thus it seems likely that the remi-induced depression of breathing rate occurs at respiratory-related neurons that are presynaptic to the preBötC neurons, which may express MORs that respond to low nanomolar opioid concentrations that are typical during clinical analgesia and respiratory depression. The sensitivity of neurons to low concentrations of opioids may not only be related to the number or density of MORs, but may also depend on the location of the MORs on the neuron. For example, if the receptors are strategically located on axon terminals, similar to the primary afferent fibers in the dorsal horn of the spinal cord that appear to inhibit the release of neurotransmitters via inhibition of voltage-dependent Ca^{2+} channels, the opioid effect could be markedly enhanced compared with a location on or near the soma.

DAMGO-induced tachypnea

Microinjections of DAMGO into the preBötC region produced an increase in respiratory rate, which was opposite to the slowing response produced by intravenous remi and also in *in vitro* studies. In brain stem slices containing the preBötC, rhythm generation appears to rely on pacemaker neuron activity (63-65). Opioid-induced membrane hyperpolarizations of pacemaker neurons produce slowing of the burst rate whereas depolarizations increase burst rate (24). Bath application of DAMGO in brain stem-spinal cord preparations (35) and systemic fentanyl in juvenile rats (P7-P-13; 16-32 g) (66) produce quantal slowing of inspiratory burst activity, while the burst rate of expiratory related activity is unchanged. Quantal slowing was not observed in this *in vivo* dog model but rather a gradual dose-dependent increase in T_I and T_E with intravenous remi. In addition, the discharge of canine expiratory neurons in the preBötC region was prolonged with remi-induced increases in T_E and remains coupled to inspiratory neuronal activity in 1:1 manner.

In developmentally mature *in vivo* preparations, rhythm generation appears to be the result of a network in which synaptic interactions among neurons play a key role (67). In such models that have been analyzed via computer simulation, the indispensable element is the reciprocal synaptic inhibition between I and E neurons with intrinsic adaptive properties that result in decrementing patterns (68). Computer simulation of such a reduced network model consisting only of I and E decrementing neurons with inhibitory reciprocal interconnections shows that a

reduction in tonic excitatory drive produces as increase in oscillatory rate, whereas an increase in excitation produces slowing due to increased synaptic inhibition (69). The drive that reaches the motoneurons is relayed via premotor neurons. At the level of the premotor neurons the tonic drive is interrupted by strong periodic inhibition from the phase-timing components of the network. This phase-timing component is believed to be located in the preBötC. Because many VRC neurons appear to express MORs (41,43), a possible explanation for the tachypnea produced by microinjection of DAMGO into the preBötC region neurons may result in decreased excitation and thus an increase in the rate of the oscillator and the respiratory rate.

Lonergan et al. microinjected endomorphine 1 into different subdivisions of the VRG and found that endomorphine 1 injected into preBötC increased the frequency of phrenic nerve discharge by 16-45%, which is similar to the data from this study. Their explanation for the increase in phrenic nerve discharge frequency following microinjection of endomorphine 1 into the preBötC may be due the removal of inhibitory inputs to the preBötC, e.g. from the BötC. Since the increase in frequency was due to changes in both expiratory and inspiratory timing, activation of the MOR by endomorphine-1 in the preBötC affects mechanisms that determine both the inspiratory on and off switches. They observed mixed effects on phrenic nerve amplitude following endomorphine-1 microinjection into the preBötC, which suggests that MORs are found on more than one type of neuron in the preBötC, or on more than one afferent input to the preBötC (70).

Possible sites for intravenous remi-induced effects

Immunohistochemical studies, using antibodies to cloned MORs have been used to examine the distribution of MORs in the rat brain. Within respiratory-related areas, the most intense MOR-like immunoreactivity (LI) was seen in the pontine lateral parabrachial nuclei (PBN), the locus coeruleus, rostral ambiguous nucleus, and the medial and commissural subnuclei of the NTS (71). The NTS contained nerve fibers with intense MOR-LI, including the primary afferent fibers of the vagus nerve. Endomorphin types 1 and 2 (EM-1 and EM-2) are endogenous peptides that have high affinity and selectivity for MORs and potent analgesic activity. Immunoreactivity to EM-1 and EM-2 was used to determine the location of fibers and cell bodies of endomorphin-containing neurons (56). In these studies, dense EM-1 LI was seen in the PBN, locus coeruleus, and the NTS. Some of the endomorphin inputs to the PBN in rats

arise from EM-1 and EM-2 LI neurons in the hypothalamus (72). Using dual labeling, immunocytochemistry combined with electron microscopy, Silverman et sl. (73) found EM-2 LI primarly in the unmyelinated axons and axon terminals. In addition, there appear to be reciprocal connections of EM-1 and EM-2 containing neurons between the hypothalamus and the NTS in the rat (74).

It is well know that inputs to the preBötC region from the NTS and the PBN contribute to respiratory phase switching. Afferent inputs from pulmonary stretch receptors end in the NTS and mediate the Breuer-Hering inspiratory inhibitory and expiratory facilitatory reflexes (75). Outputs from the neurons in the parabrachial complex region, including the Kölliker-Fuse nucleus and intertrigeminal region project to the VRC, and chemical or electrical activation of these neurons profoundly alter respiratory phase timing (76). A recent network model, which assigns specific synaptic connections between pontine neurons and preBötC/Bötzinger neurons, is able to simulate experimentally observed responses to various perturbations (68). Thus it appears that the presence of dense MORs in the PBN and NTS suggest that they could be potential sites where systemic opioids such as intravenous remi act to produce their effect on breathing rate. Another possible site may include the midline medullary raphe region where MOR LI has been seen (71). Zhang et coworker found that the systemic DAMGO induced inhibition of ventilation and of the carbon dioxide response was significantly reduced after pretreatment of the caudal raphe region with a selective MOR antagonist (77).

6. CONCLUSIONS

This study indicates that remifentanil at clinically relevant plasma concentrations (19.4±1.2 nM) does not cause respiratory depression via μ-opioid receptor activation in the preBötC, the putative rhythm generating center.

In contrast, activation of MORs within of the preBötC region produces tachypnea in vivo. The tachypnea produced by DAMGO microinjections into the preBötC may be due to a reduced excitation between rhythmogenic neurons, which may result in the increased rate of the central rhythm generator.

It is possible that the bradypnea induced by systemic opioids may originate from μ-opioid receptor activation on presynaptic neurons outside the preBötC region, which supply inputs to the preBötC and indirectly alter rhythm.

By eliminating the preBötC as the site of bradypnea induced by systemically administered opioid agonists in the canine *in vivo* model, this study has provided the groundwork for future studies. An extension of this study in the same canine in vivo model has just now shown that the MORs in the parabrachial region of the rostral dorsal lateral pons are primarily, and possibly solely, responsible for bradypnea induced by intravenous remifentanil (78).

7. SUMMARY

AIM: Systemic administration of μ-opioids at clinical doses for analgesia typically decreases respiratory rate. MORs on preBötC respiratory neurons, the putative kernel of respiratory rhythmogenesis, are potential targets. The purpose of this study was to determine the contribution of the preBötC MORs to the bradypnea produced in vivo by intravenous administration of clinically relevant infusion rates of remifentanil, a short-acting, potent μ-opioid analgesic.

METHODS: In decerebrate dogs, multibarrel micropipettes were used to record preBötC neuronal activity and to eject the opioid antagoinist naloxone (NAL, 0.5 mM), the glutamate agonist D-homocysteic acid (DLH, 20 mM), or the MOR agonist ($_{D}$-Ala^{2}, N-Me-Phe^{4}, gly-ol^{5})-enkephalin (DAMGO, 100 μM). Inspiratory and expiratory durations (T_I and T_E) and peak phrenic nerve activity (PPA) were measured from the phrenic neurogram. The preBötC was functionally identified by its rate altering response (typically tachypnea) to DLH microinjection and neuron composition.

RESULTS: During intravenous remi-induced bradypnea (~60% decrease in central breathing frequency, f_B), bilateral injections of NAL into the preBötC did not change T_I, T_E, f_B, and PPA. Also, NAL picoejected onto single preBötC neurons depressed by intravenous remi had no effect on their discharge. In contrast, ~60 μg/kg of intravenous NAL rapidly reversed all remi-induced effects. In a separate group of dogs, microinjections of DAMGO in the preBötC increased f_B by 44%, while subsequent intravenous remi infusion more than offset this DAMGO induced tachypnea.

CONCLUSION: These results indicate that μ-opioids at plasma concentrations that cause profound analgesia produced their bradypneic effect via MORs located outside the preBötC region.

8. REFERENCES

1. Lalley PM. Opioidergic and dopaminergic modulation of respiration. Respir Physiol Neurobiol 2008;164:160-7.
2. Alheid GF, McCrimmon DR. The chemical neuroanatomy of breathing. Respir Physiol Neurobiol 2008;164:3-11.
3. Stornetta RL. Identification of neurotransmitters and co-localization of transmitters in brainstem respiratory neurons. Respir Physiol Neurobiol 2008;164:18-27.
4. Dobbins EG, Feldman JL. Brainstem network controlling descending drive to phrenic motoneurons in rat. J Comp Neurol 1994;347:64-86.
5. Guyenet PG, Sevigny CP, Weston MC, Stornetta RL. Neurokinin-1 receptor-expressing cells of the ventral respiratory group are functionally heterogeneous and predominantly glutamatergic. J Neurosci 2002;22:3806-16.
6. Stornetta RL, Sevigny CP, Guyenet PG. Inspiratory augmenting bulbospinal neurons express both glutamatergic and enkephalinergic phenotypes. J Comp Neurol 2003;455:113-24.
7. Alheid GF, Gray PA, Jiang MC, Feldman JL, McCrimmon DR. Parvalbumin in respiratory neurons of the ventrolateral medulla of the adult rat. J Neurocytol 2002;31:693-717.
8. Feldman JL, Del Negro CA. Looking for inspiration: new perspectives on respiratory rhythm. Nat Rev Neurosci 2006;7:232-42.
9. Onimaru H, Homma I. A novel functional neuron group for respiratory rhythm generation in the ventral medulla. J Neurosci 2003;23:1478-86.
10. Tian GF, Peever JH, Duffin J. Botzinger-complex expiratory neurons monosynaptically inhibit phrenic motoneurons in the decerebrate rat. Exp Brain Res 1998;122:149-56.
11. Ezure K, Tanaka I, Kondo M. Glycine is used as a transmitter by decrementing expiratory neurons of the ventrolateral medulla in the rat. J Neurosci 2003;23:8941-8.
12. Krolo M, Stuth EA, Tonkovic-Capin M, Hopp FA, McCrimmon DR, Zuperku EJ. Relative magnitude of tonic and phasic synaptic excitation of medullary inspiratory neurons in dogs. Am J Physiol Regul Integr Comp Physiol 2000;279:R639-49.

13. Smith JC, Abdala AP, Rybak IA, Paton JF. Structural and functional architecture of respiratory networks in the mammalian brainstem. Philos Trans R Soc Lond B Biol Sci 2009;364:2577-87.
14. Smith JC, Ellenberger HH, Ballanyi K, Richter DW, Feldman JL. Pre-Botzinger complex: a brainstem region that may generate respiratory rhythm in mammals. Science 1991;254:726-9.
15. Guyenet PG, Wang H. Pre-Botzinger neurons with preinspiratory discharges "in vivo" express NK1 receptors in the rat. J Neurophysiol 2001;86:438-46.
16. Koshiya N, Smith JC. Neuronal pacemaker for breathing visualized in vitro. Nature 1999;400:360-3.
17. Johnson SM, Koshiya N, Smith JC. Isolation of the kernel for respiratory rhythm generation in a novel preparation: the pre-Botzinger complex "island". J Neurophysiol 2001;85:1772-6.
18. Lieske SP, Thoby-Brisson M, Telgkamp P, Ramirez JM. Reconfiguration of the neural network controlling multiple breathing patterns: eupnea, sighs and gasps [see comment]. Nat Neurosci 2000;3:600-7.
19. Del Negro CA, Morgado-Valle C, Hayes JA, Mackay DD, Pace RW, Crowder EA, Feldman JL. Sodium and calcium current-mediated pacemaker neurons and respiratory rhythm generation. J Neurosci 2005;25:446-53.
20. Ramirez JM, Tryba AK, Pena F. Pacemaker neurons and neuronal networks: an integrative view. Curr Opin Neurobiol 2004;14:665-74.
21. Doi A, Ramirez JM. Neuromodulation and the orchestration of the respiratory rhythm. Respir Physiol Neurobiol 2008;164:96-104.
22. Bianchi AL, Denavit-Saubie M, Champagnat J. Central control of breathing in mammals: neuronal circuitry, membrane properties, and neurotransmitters. Physiol Rev 1995;75:1-45.
23. Liu YY, Wong-Riley MT, Liu JP, Wei XY, Jia Y, Liu HL, Fujiyama F, Ju G. Substance P and enkephalinergic synapses onto neurokinin-1 receptor-immunoreactive neurons in the pre-Botzinger complex of rats. Eur J Neurosci 2004;19:65-75.

24. Gray PA, Rekling JC, Bocchiaro CM, Feldman JL. Modulation of respiratory frequency by peptidergic input to rhythmogenic neurons in the preBotzinger complex. Science 1999;286:1566-8.
25. Stuth EAE SA, Zuperku EJ Central effects of general anesthesia. In: Ward DS DA, Teppema LJ, Boca Raton, ed. Pharmacology and Pathophysiology of the Control of Breathing: FL: Taylor and Francis, 2005:571-652.
26. Ezure K, Tanaka I. Distribution and medullary projection of respiratory neurons in the dorsolateral pons of the rat. Neuroscience 2006;141:1011-23.
27. Pattinson KT. Opioids and the control of respiration. Br J Anaesth 2008;100:747-58.
28. Montandon G, Qin W, Liu H, Ren J, Greer JJ, Horner RL. PreBotzinger complex neurokinin-1 receptor-expressing neurons mediate opioid-induced respiratory depression. J Neurosci;31:1292-301.
29. Cashman JN, Dolin SJ. Respiratory and haemodynamic effects of acute postoperative pain management: evidence from published data. Br J Anaesth 2004;93:212-23.
30. Le Merrer J, Becker JA, Befort K, Kieffer BL. Reward processing by the opioid system in the brain. Physiol Rev 2009;89:1379-412.
31. Janecka A, Fichna J, Janecki T. Opioid receptors and their ligands. Curr Top Med Chem 2004;4:1-17.
32. Pan HL, Wu ZZ, Zhou HY, Chen SR, Zhang HM, Li DP. Modulation of pain transmission by G-protein-coupled receptors. Pharmacol Ther 2008;117:141-61.
33. Al-Hasani R. Molecular Mechanisms of Opioid Receptor-dependent Signaling and Behavior. Anesthesiology 2011;115:1363-81.
34. Johnson SM, Smith JC, Feldman JL. Modulation of respiratory rhythm in vitro: role of Gi/o protein-mediated mechanisms. J Appl Physiol 1996;80:2120-33.
35. Mellen NM, Janczewski WA, Bocchiaro CM, Feldman JL. Opioid-induced quantal slowing reveals dual networks for respiratory rhythm generation. Neuron 2003;37:821-6.
36. Gray PA, Janczewski WA, Mellen N, McCrimmon DR, Feldman JL. Normal breathing requires preBotzinger complex neurokinin-1 receptor-expressing neurons. Nat Neurosci 2001;4:927-30.

37. Krolo M, Tonkovic-Capin V, Stucke AG, Stuth EA, Hopp FA, Dean C, Zuperku EJ. Subtype composition and responses of respiratory neurons in the pre-botzinger region to pulmonary afferent inputs in dogs. J Neurophysiol 2005;93:2674-87.
38. Monnier A, Alheid GF, McCrimmon DR. Defining ventral medullary respiratory compartments with a glutamate receptor agonist in the rat. J Physiol 2003;548:859-74.
39. Haji A, Yamazaki H, Ohi Y, Takeda R. Distribution of mu receptors in the ventral respiratory group neurons; immunohistochemical and pharmacological studies in decerebrate cats. Neurosci Lett 2003;351:37-40.
40. Lalley PM. Mu-opioid receptor agonist effects on medullary respiratory neurons in the cat: evidence for involvement in certain types of ventilatory disturbances. Am J Physiol Regul Integr Comp Physiol 2003;285:R1287-304.
41. Manzke T, Guenther U, Ponimaskin EG, Haller M, Dutschmann M, Schwarzacher S, Richter DW. 5-HT4(a) receptors avert opioid-induced breathing depression without loss of analgesia. Science 2003;301:226-9.
42. Lalley PM. D1-dopamine receptor agonists prevent and reverse opiate depression of breathing but not antinociception in the cat. Am J Physiol Regul Integr Comp Physiol 2005;289:R45-51.
43. Stucke AG, Zuperku EJ, Sanchez A, Tonkovic-Capin M, Tonkovic-Capin V, Mustapic S, Stuth EA. Opioid receptors on bulbospinal respiratory neurons are not activated during neuronal depression by clinically relevant opioid concentrations. J Neurophysiol 2008;100:2878-88.
44. Chitravanshi VC, Sapru HN. Phrenic nerve responses to chemical stimulation of the subregions of ventral medullary respiratory neuronal group in the rat. Brain Res 1999;821:443-60.
45. Connelly CA, Dobbins EG, Feldman JL. Pre-Botzinger complex in cats: respiratory neuronal discharge patterns. Brain Res 1992;590:337-40.
46. Sun QJ, Goodchild AK, Chalmers JP, Pilowsky PM. The pre-Botzinger complex and phase-spanning neurons in the adult rat. Brain Res 1998;809:204-13.
47. Chitravanshi VC, Sapru HN. GABA receptors in the phrenic nucleus of the rat. Am J Physiol 1999;276:R420-8.

48. Solomon IC, Edelman NH, Neubauer JA. Patterns of phrenic motor output evoked by chemical stimulation of neurons located in the pre-Botzinger complex in vivo. J Neurophysiol 1999;81:1150-61.
49. Wang H, Germanson TP, Guyenet PG. Depressor and tachypneic responses to chemical stimulation of the ventral respiratory group are reduced by ablation of neurokinin-1 receptor-expressing neurons. J Neurosci 2002;22:3755-64.
50. Servin FS, Billard V. Remifentanil and other opioids. Handb Exp Pharmacol 2008:283-311.
51. Burkle H, Dunbar S, Van Aken H. Remifentanil: a novel, short-acting, mu-opioid. Anesth Analg 1996;83:646-51.
52. Michelsen LG, Hug CC, Jr. The pharmacokinetics of remifentanil. J Clin Anesth 1996;8:679-82.
53. Michelsen LG, Salmenpera M, Hug CC, Jr., Szlam F, VanderMeer D. Anesthetic potency of remifentanil in dogs. Anesthesiology 1996;84:865-72.
54. Nicholson C. Diffusion from an injected volume of a substance in brain tissue with arbitrary volume fraction and tortuosity. Brain Res 1985;333:325-9.
55. Motulsky H. Intuitive Biostatistics. New York: Oxford, 1995.
56. Martin-Schild S, Gerall AA, Kastin AJ, Zadina JE. Differential distribution of endomorphin 1- and endomorphin 2-like immunoreactivities in the CNS of the rodent. J Comp Neurol 1999;405:450-71.
57. Zadina JE, Martin-Schild S, Gerall AA, Kastin AJ, Hackler L, Ge LJ, Zhang X. Endomorphins: novel endogenous mu-opiate receptor agonists in regions of high mu-opiate receptor density. Ann N Y Acad Sci 1999;897:136-44.
58. Bruns D, Riedel D, Klingauf J, Jahn R. Quantal release of serotonin. Neuron 2000;28:205-20.
59. Clements JD. Transmitter timecourse in the synaptic cleft: its role in central synaptic function. Trends Neurosci 1996;19:163-71.
60. Lieske SP, Thoby-Brisson M, Telgkamp P, Ramirez JM. Reconfiguration of the neural network controlling multiple breathing patterns: eupnea, sighs and gasps. Nat Neurosci 2000;3:600-7.

61. Gharagozlou P, Demirci H, David Clark J, Lameh J. Activity of opioid ligands in cells expressing cloned mu opioid receptors. BMC Pharmacol 2003;3:1.
62. Kalvass JC, Olson ER, Pollack GM. Pharmacokinetics and pharmacodynamics of alfentanil in P-glycoprotein-competent and P-glycoprotein-deficient mice: P-glycoprotein efflux alters alfentanil brain disposition and antinociception. Drug Metab Dispos 2007;35:455-9.
63. Ballanyi K, Onimaru H, Homma I. Respiratory network function in the isolated brainstem-spinal cord of newborn rats. Prog Neurobiol 1999;59:583-634.
64. Butera RJ, Jr., Rinzel J, Smith JC. Models of respiratory rhythm generation in the pre-Botzinger complex. I. Bursting pacemaker neurons. J Neurophysiol 1999;82:382-97.
65. Butera RJ, Jr., Rinzel J, Smith JC. Models of respiratory rhythm generation in the pre-Botzinger complex. II. Populations Of coupled pacemaker neurons. J Neurophysiol 1999;82:398-415.
66. Janczewski WA, Feldman JL. Distinct rhythm generators for inspiration and expiration in the juvenile rat. J Physiol 2006;570:407-20.
67. Richter DW, Spyer KM. Studying rhythmogenesis of breathing: comparison of in vivo and in vitro models. Trends Neurosci 2001;24:464-72.
68. Rybak IA, O'Connor R, Ross A, Shevtsova NA, Nuding SC, Segers LS, Shannon R, Dick TE, Dunin-Barkowski WL, Orem JM, Solomon IC, Morris KF, Lindsey BG. Reconfiguration of the pontomedullary respiratory network: a computational modeling study with coordinated in vivo experiments. J Neurophysiol 2008;100:1770-99.
69. Stuth EAE, Stucke AG, Zuperku RJ. Central effects of general anesthesia. In: Pharmacology and Pathophysiology of the Control of Breathing, edited by Ward DS, Dahan A, Teppema lj. Boca Raton, FL: Taylor and Francis, 2005, chap 15, p. 571-652.
70. Lonergan T, Goodchild AK, Christie MJ, Pilowsky PM. Mu opioid receptors in rat ventral medulla: effects of endomorphin-1 on phrenic nerve activity. Respir Physiol Neurobiol 2003;138:165-78.
71. Ding YQ, Kaneko T, Nomura S, Mizuno N. Immunohistochemical localization of mu-opioid receptors in the central nervous system of the rat. J Comp Neurol 1996;367:375-402.

72. Chen T, Hui R, Dong YX, Li YQ, Mizuno N. Endomorphin 1- and endomorphin 2-like immunoreactive neurons in the hypothalamus send axons to the parabrachial nucleus in the rat. Neurosci Lett 2004;357:139-42.
73. Silverman MB, Hermes SM, Zadina JE, Aicher SA. Mu-opioid receptor is present in dendritic targets of Endomorphin-2 axon terminals in the nuclei of the solitary tract. Neuroscience 2005;135:887-96.
74. Hui R, Chen T, Li YQ. The reciprocal connections of endomorphin 1- and endomorphin 2-containing neurons between the hypothalamus and nucleus tractus solitarii in the rat. Neuroscience 2006;138:171-81.
75. Kubin L, Alheid GF, Zuperku EJ, McCrimmon DR. Central pathways of pulmonary and lower airway vagal afferents. J Appl Physiol 2006;101:618-27.
76. Chamberlin NL. Functional organization of the parabrachial complex and intertrigeminal region in the control of breathing. Respir Physiol Neurobiol 2004;143:115-25.
77. Zhang Z, Xu F, Zhang C, Liang X. Activation of opioid mu receptors in caudal medullary raphe region inhibits the ventilatory response to hypercapnia in anesthetized rats. Anesthesiology 2007;107:288-97.
78. Prkic I, Mustapic S, Radocaj T, Stucke AG, Stuth EA, Hopp FA, Dean C, Zuperku EJ. Pontine mu-opioid receptors mediate the bradypnea caused by intravenous remifentanil infusions at clinically relevant concentrations in dogs. J Neurophysiol 2012.

9. CURRICULUM VITAE

Sanda Mustapić, M.D.

Date and Place of Birth: April 24, 1980., Split, Croatia

Work Address:

Department of gastroenterology, Clinical Hospital Dubrava

10 000 Zagreb, Croatia.

e-mail: sanda.mustapic@mefst.hr

EDUCATION:

1998-2004.: University of Mostar, School of Medicine, Bosnia and Hercegovina

2006.: Board exam

2010 –present: Postgraduate school "Translational research in biomedicine (TRIBE)"

University of Split, School of Medicine Split, Croatia.

WORK EXPERIENCE:

2005-2006.: Internship, Split, Croatia

2006-2010.: Postdoctoral research fellow, Medical College of Wisconsin, Milwaukee, WI, USA

2010-2012.: Research fellow, University of Split, Shool of Medicine Split, Croatia

10/2010-01/2011.: Postdoctoral research fellow, Medical College of Wisconsin, Milwaukee, WI, USA

02/2012. - present: Resident of internal medicine, Clinical Hospital Dubrava, Zagreb, Croatia.

PUBLICATIONS:

1. Astrid G. Stucke, Edward J. Zuperku, Antonio Sanchez, Mislav Tonkovic-Capin, Viseslav Tonkovic-Capin, **Sanda Mustapic** and Eckehard A. Stuth. Opioid receptors on bulbospinal respiratory neurons are not activated during neuronal depperssion by clinically relevant opioid concetrations, J Neurophysiol 100 2878-2888, 2008; doi:10.1152/jn.90620.2008.

2. Antonio Sanchez, **Sanda Mustapic**, Edward J. Zuperku, Astrid G. Stucke, Francis A. Hopp, and Eckehard A. E. Stuth. Role of inhibitory neurotransmission in the control of canine hypoglossal motoneuron activity in vivo, J Neurophysiol 101:1211-1221, 2009; doi:10.1152/jn.90279.2008.
3. **Sanda Mustapic**, Tomislav Radocaj, Antonio Sanchez, Zoran Dogas, Astrid Stucke, Francis Hopp, Eckehard Stuth, and Edward Zuperku. Clinically relevant infusion rates of μ-opioid remifentanil causes bradypnea in decerebrate dogs but not via direct effects in the pre-Bötzinger Complex Region, J Neurophysiol 103:409-418, 2010; doi:10.1152/jn.00188.2009.

4. Prkic Ivana, **Mustapic Sanda**, Radocaj Tomislav, Stucke Astrid G, Stuth Eckehard A.E, Hopp Francis A., Dean Caron, and Zuperku Edward J. Pontine μ-opioid receptors mediate the bradypnea caused by intravenous remifentanil infusions at clinically relevant concentrations in dogs. J Neurophysiol 2012; doi: 10.1152/jn.00185.2012.

POSTERS AND PRESENTATIONS AT SCIENTIFIC MEETINGS:

1. Antonio Sanchez, **Sanda Mustapic**, Astrid G. Stucke, Francis A. Hopp, Zoran Dogas, Edward J. Zuperku and Eckehard A. Stuth. Endogenous $GABA_A$ receptor-mediated attenuation of hypoglossal motoneuronal discharge activity in vivo. Experimental Biology 2007, Washington D.C., USA, April 2007.
2. Antonio Sanchez, Eckehard A. E. Stuth, **Sanda Mustapic**, Astrid G. Stucke and Edward J Zuperku. GABA, not glycine, contributes to synaptic inhibition of inspiratory hypoglossal motoneurons in vivo. American Society of Anesthesiologists 2007, San Francisco, CA, USA, October 2007.
3. Astrid G. Stucke, Edward J. Zuperku, Antonio Sanchez, **Sanda Mustapic** and Eckehard A. Stuth. Remifentanil depresses respiratory premotor neurons but not via opioid receptors on these neurons. American Society of Anesthesiologists 2007, San Francisco, CA, USA, October 2007.
4. **Sanda Mustapic**, Antonio Sanchez, Astrid G. Stucke, Eckehard A. E. Stuth, and Edward J Zuperku. Depression of respiratory rate by intravenous opioids is not due to direct

opioid effects on neurons within the preBötzinger Complex (pBC) region. Experimental Biology 2008, San Diego, CA, USA, April 2008.

5. Antonio Sanchez, **Sanda Mustapic**, Astrid G. Stucke, Edward J. Zuperku, and Eckehard A. E. Stuth. Contribution of synaptic inhibition to the control of inspiratory hypoglossal motorneuronal (IHMN) activity *in vivo*. Experimental Biology 2008, San Diego, CA, USA, April 2008.
6. Astrid G. Stucke, **Sanda Mustapic**, Antonio Sanchez, Zoran Dogas, Eckehard A. E. Stuth, and Edward J. Zuperku. Developmental changes in the pattern of the hypoxic ventilatory response in rabbits. Experimental Biology 2008, San Diego, CA, USA, April 2008.
7. Astrid G. Stucke, Eckehard A. E. Stuth, **Sanda Mustapic**, Zoran Dogas, Edward J. Zuperku. Maturation of the acute hypoxic ventilatory response during volatile anesthesia in rabbits. American Society of Anesthesiologist 2008, Orlando, FL, USA, October 2008.
8. **Sanda Mustapic**, Eckehard, A. E. Stuth, Tomislav Radocaj, Astrid G. Stucke, Edward J. Zuperku. Does the pre-Bötzinger Complex (pBC) mediate the bradypnea caused by intravenous opioids? American Society of Anesthesiologist 2008, Orlando, FL, USA, October 2008.
9. **Sanda Mustapic**, Tomislav Radocaj, Astrid G. Stucke, Eckehard A. E. Stuth, Zoran Dogas, and Edward J. Zuperku. Local microinjection of μ-opioids into the pre-Bötzinger complex (pre-BöC) region produces opposite effects on breathing rate to systemic μ-opioid infusion in decerebrate dogs. Experimental Biology 2009, New Orleans, LA, USA, April 2009.
10. Tomisalv Radocaj, **Sanda Mustapic**, Astrid G. Stucke, Eckehard A. E. Stuth, and Edward J. Zuperku. Effects of local microinjection of biogenic amines into the pre-Bötzinger complex (pBC) and adjacent ventral respiratory column (VCR) on the canine breathing pattern. Experimental Biology 2009, New Orleans, LA, USA, April 2009.
11. **Sanda Mustapic**, Eckehard A. E. Stuth, Tomislav Radocaj, Edward Zuperku, and Astrid G. Stucke. Direct micoejection of μ-opioids into preBötzinger complex region in vivo produces tachypnea. American Society of Anesthesiologist 2009, New Orleans, LA, USA, October 2009.

12. **Sanda Mustapic,** Tomislav Radocaj, Astrid G. Stucke, Eckehard A. E. Stuth, Zoran Dogas, Francis A. Hopp, Edward J. Zuperku. Effects of IV Remifentanil (Remi) on the discharge patterns of canine preBötzinger complex (pBC) neurons. Experimental Biology 2010, Anaheim, CA, USA, April 2010.
13. Tomislav Radocaj, **Sanda Mustapic**, Astrid G. Stucke, Eckehard A. E. Stuth and Edward J. Zuperku. Dose-dependent depression of the preBötzinger Complex (pBC) region neurons by local application of the 5HT1A receptor agonist 8OH-DPAT. Experimental Biology 2010, Anaheim, CA, USA, April 2010.
14. Astrid G. Stucke, Eckehard A. E. Stuth, **Sanda Mustapic**, Tomislav Radocaj, Edward J. Zuperku. Changes in CO_2 during acute hypoxia in immature and adult rabbits and the development of apnea. Experimental Biology 2010, Anaheim, CA, USA, April 2010.
15. Tomislav Radocaj, Eckehard A. E. Stuth, **Sanda Mustapic**, Astrid G. Stucke, Edward J. Zuperku. Do noradrenergic inputs contribute to hypoglossal motoneuron activity in decerebrate dogs? American Society of Anesthesiologist 2010, San Diego, CA, USA, October 2010.
16. Eckehard A. E. Stuth, Tomislav Radocaj, **Sanda Mustapic**, Astrid G. Stucke, Francis A. Hopp, Edward J. Zuperku. Noradrenergic inputs to inspiratory hypoglossal motoneurons (IHMN) in decerebrate dogs. Experimental Biology 2011, Washington D.C., USA, April 2011.
17. Ivana Prkic, **Sanda Mustapic**, Tomislav Radocaj, Astrid G. Stucke, Eckehard A. E. Stuth, Francis A. Hopp, Caron Dean and Edward J. Zuperku. Pontine μ-opioid receptors mediate the bradypnea caused by clinically relevant rates of intravenous remifentanil in dogs. Experimental Biology 2012, San Diego, USA, April 2012.
18. **Sanda Mustapic**, Zarko Babic, Marko Banic, Ivica Grgurevic, Mirjana Vukelic-Markovic, Tajana Stoos-Veic, and Milan Kujundzic. Pancreatic and peripancreatic mass as a presentation of intra-abdominal tuberculosis: a case report. 7^{th} Central European Gastroenterology Meeting, Cluj-Napoca, Romania, 27-29 September 2012.

ORAL PRESENTATIONS AT SCIENTIFIC MEETINGS:

1. **Sanda Mustapic**, Do μ-opioid receptors within the preBotzinger complex contribute to the bradypnea produced by systemic administration of mu-opioids at clinical doses, in vivo? 42nd Annual Control of Respiration Mixer-2008. 'Hot Topics in Respiratory Control", Experimental Biology, San Diego, CA, USA, April 2008.
2. **Sanda Mustapic**, What are the effects of local microinjection of the selective μ-opioid agonist DAMGO into the pre Botzinger complex? 43rd Annual Control of Respiration Mixer-2009. 'Hot Topics in Respiratory Control", Experimental Biology, New Orleans, LA, USA, April 2009.

MEMBERSHIP:

Member of the Croatian Medical Association.